# Małe, średnie i ... nano. Modelowanie molekularne w Opolu (i nie tylko)

**Badania podstawowe wspomagane obliczeniami w WCSS**


## Teobald Kupka, Małgorzata A. Broda

*Uniwersytet Opolski, Wydział Chemii, Opole*

*e-mail: teobaldk@yahoo.com; broda@uni.opole.pl*


*WCSS Wrocław, 11.02.2014*

# Autor


**Dr hab. Teobald Kupka, prof. U. O.**
Uniwersytet Opolski
Wydział Chemii
Ul. Oleska 48, 45-052 Opole
teobaldk@gmail.com
Tel. 665 921 475

# WPROWADZENIE

1. Wstęp
2. Bilans roku 2013
3. Szczegóły
4. Problematyka naukowa
5. Podziękowania

# BILANS ROKU 2013

**Publikacje:**

| | |
|---|---|
| **Opublikowane** | **5 +** |
| **Wysłane** | **3** |
| **Razem** | **9** |

**Ponadto:**

| | |
|---|---|
| **Komunikaty** | **20** |
| **Prace magisterskie** | **4** |
| **Prace doktorskie (kontynuacja + nowe)** | **4 + 3** |

# Prace opublikowane w 2013 roku

1. **T. Kupka*, M. Stachów, E. Chełmecka, K. Pasterny, M. Stobińska, L. Stobiński and J. Kaminsky,**
   **Efficient Modeling of NMR Parameters in Carbon Nanosystems**
   **J. Chem. Theor. Comput., 9 (2013) 4275 – 4286 (IF = 5.389 w 2012).**

2. **T. Kupka*, M. Stachów, J. Kaminsky and L. Stobiński,**
   **$^{3}$He NMR: from free gas to its encapsulation in fullerene,**
   **Magn. Reson. Chem., 51 (2013) 463 – 468. (IF = 1.528 w 2012).**

3. **T. Kupka*, M. Stachów, J. Kaminsky and S.P.A Sauer*,**
   **Estimation of isotropic nuclear magnetic shieldings in the CCSD(T) and MP2 complete basis set limit using affordable correlation calculations,**
   **Magn. Reson. Chem., 51 (2013) 482 – 489. (IF = 1.528 w 2012).**

4. **K. Radula-Janik, T. Kupka*, K. Ejsmont, Z. Daszkiewicz and S. P. A. Sauer,**

   **Halogen effect on structure and 13C NMR chemical shift of 3,6-disubstituted-*N*-alkyl carbazoles,**
   ***Magn. Reson. Chem. 51 (2013) 630-635. October* , DOI: 10.1002/mrc.3992 *(IF=1.528 in 2012).***

5. **T. Kupka*, M. Nieradka, J. Kaminský and L. Stobiński,**
   **Modeling 21Ne NMR parameters for carbon nanosystems,**
   ***Magn. Reson. Chem., 51 (2013) 676-681* (IF=1.528 in 2012).**

---

# Prace opublikowane online w 2013 roku

1. **T. Kupka*, M. Stachów, M. Nieradka, K. Radula-Janik, L. Stobiński, J. Kaminský*,**
   **From Small to Medium and Beyond. A Pragmatic Approach in Predicting Properties of Ne Containing Structures**
   **Mol. Phys. – DOI:10.1080/00268976.2013.848301 (IF=1.670 in 2012, cyt. = 0). Published online: 28 Oct 2013.**

2. **A. Buczek, M. Makowski, M. Jewgiński, R. Latajka, T. Kupka, M. A. Broda*,**
   **Toward engineering efficient peptidomimetics. Screening conformational landscape of two modified dehydroaminoacids,**
   ***Biopolymers, 101 (2014) 28-40.* DOI: 10.1002/bip.22264 *(IF = 2.879 in 2012).***

---

**B.**

**Oprogramowanie i sprzęt WCSS pozwoliły również na zakończenie jednej pracy magisterskiej i rozpoczęcie dwóch kolejnych.**

**C.**

**Ponadto 20 wystąpień opierało się na materiale obliczeniowym uzyskanym zarówno w WCSS i w Cyfronecie.**

ROK 2013

Research Article

Magnetic Resonance in Chemistry

Received: 10 April 2013 Revised: 12 May 2013 Accepted: 14 May 2013 Published online in Wiley Online Library: 10 June 2013

(wileyonlinelibrary.com) DOI 10.1002/mrc.3974

# Estimation of isotropic nuclear magnetic shieldings in the CCSD(T) and MP2 complete basis set limit using affordable correlation calculations

Teobald Kupka,[a]* Michał Stachów,[a,b] Jakub Kaminsky[c] and Stephan P. A. Sauer[d]**

**A linear correlation between isotropic nuclear magnetic shielding constants for seven model molecules ($CH_2O$, $H_2O$, HF, $F_2$, HCN, $SiH_4$ and $H_2S$) calculated with 37 methods (34 density functionals, RHF, MP2 and CCSD(T)), with affordable pcS-2 basis set and corresponding complete basis set results, estimated from calculations with the family of polarization-consistent pcS-*n* basis sets is reported. This dependence was also supported by inspection of profiles of deviation between CBS estimated nuclear shieldings and shieldings obtained with the significantly smaller basis sets pcS-2 and aug-cc-pVTZ-J for the selected set of 37 calculation methods. It was possible to formulate a practical approach of estimating the values of isotropic nuclear magnetic shielding constants at the CCSD(T)/CBS and MP2/CBS levels from affordable CCSD(T)/pcS-2, MP2/pcS-2 and DFT/CBS calculations with pcS-n basis sets. The proposed method leads to a fairly accurate estimation of nuclear magnetic shieldings and considerable saving of computational efforts.** 

*Supporting information may be found in the online version of this article.*

**Keywords:** isotropic nuclear magnetic shielding; CBS; CCSD(T); pcS-2; aug-cc-pVTZ-J; DFT

**Table 1.** Experimental and empirical[a] nuclear magnetic shieldings of nonhydrogen atoms in the model molecules obtained using our ZPV correction (at BHandH/pcS-3 level and added temperature correction (TC) value from literature)

| Nuclei/ Molecule | Exp. | ZPVC (pcS-2) | ZPVC (pcS-3) | ZPVC (Lit.) | Emp. (This work) | Equil. [+ ZPV + TC] (Lit.) |
|---|---|---|---|---|---|---|
| **$^{13}C$ in $CH_2O$** | $-4.4 \pm 3$[bc] | −9.34 | −8.57 | −2.46[d] | 4.17 | 2.8[e], 4.7[f] |
| **$^{13}C$ in HCN** | 82.1[g] | −3.28 | −3.15 | −1.62[h] | 85.25 | 85.0[i]; 86.3[j] |
| **$^{15}N$ in HCN** | −20.4[g] | −14.03 | −13.25 | −8.2[k] | −7.15 | −13.3[l]; -13.6[j] |
| **$^{17}O$ in $CH_2O$** | $-375 \pm 100$[b] $-427 \pm 100$[b] | −50.49 | −45.44 | | −420.44 | −383.1[f] |
| **$^{17}O$ in $H_2O$** | **325.3** $\pm 0.3$[m] | −10.28 | **−10.19** | −10.93[o], | **335.89** | 337.69[u] |
| | $323.6 \pm 0.6$[n] | | | −11.72[o] | | |
| | | | | **−0.4**[p] | | |
| | | | | −10.3[r] | | |
| | | | | −9.3[s] | | |
| | | | | −10.93[t] | | |
| **$^{19}F$ in $F_2$** | −233.2[v] | −16.64 | −15.98 | −20.77[w] | −217.22 | −214.9[x] |
| **$^{19}F$ in HF** | $409.6 \pm 1.0$[y] | −8.70 | **−8.75** | −8.22[z], | 418.69 | 410.3[a1] |
| | | | | −8.11[z] | | |
| **$^{29}Si$ in $SiH_4$** | $482.846 \pm 5.0$[b1] | 9.19 | 7.81 | −1.409[d1] | 475.036 | 469.236[e1] |
| | $475.3 \pm 10$[c1] | | | | | |
| **$^{33}S$ in $H_2S$** | $726.0 \pm 2$[f1] | −18.44 | **−17.90** | −20.859[g1] | **726.759**[h1] | 738.990[i1] |

**Table 2.** RMS values of the selected nuclear shieldings deviations calculated with 34 density functionals, RHF and MP2 for individual basis set and CBS from the corresponding experimental (empirical) values

| Molecular system | Basis set | | | | |
|---|---|---|---|---|---|
| | aug-cc-pVTZ-J | pcS-2 | pcS-3 | pcS-4 | CBS |
| **C in $CH_2O$** | 19.193 | 25.075 | 25.834 | 25.949 | 26.033 |
| **O in $CH_2O$** | 51.435 | 75.035 | 69.257 | 69.158 | 69.065 |
| **F in $F_2$** | 29.516 | 37.824 | 40.734 | 41.574 | 42.164 |
| **F in HF** | 5.758 | 6.163 | 7.257 | 7.101 | 6.989 |
| **O in $H_2O$** | 6.747 | 6.939 | 8.549 | 8.507 | 8.476 |
| **C in HCN** | 10.794 | 15.164 | 15.559 | 15.633 | 15.687 |
| **N in HCN** | 31.236 | 40.126 | 39.749 | 39.836 | 39.901 |
| **Si in $SiH_4$** | 17.120 | 26.939 | 29.416 | 29.377 | 29.350 |
| **S in $H_2S$** | 15.000 | 16.871 | 17.025 | 17.218 | 17.373 |

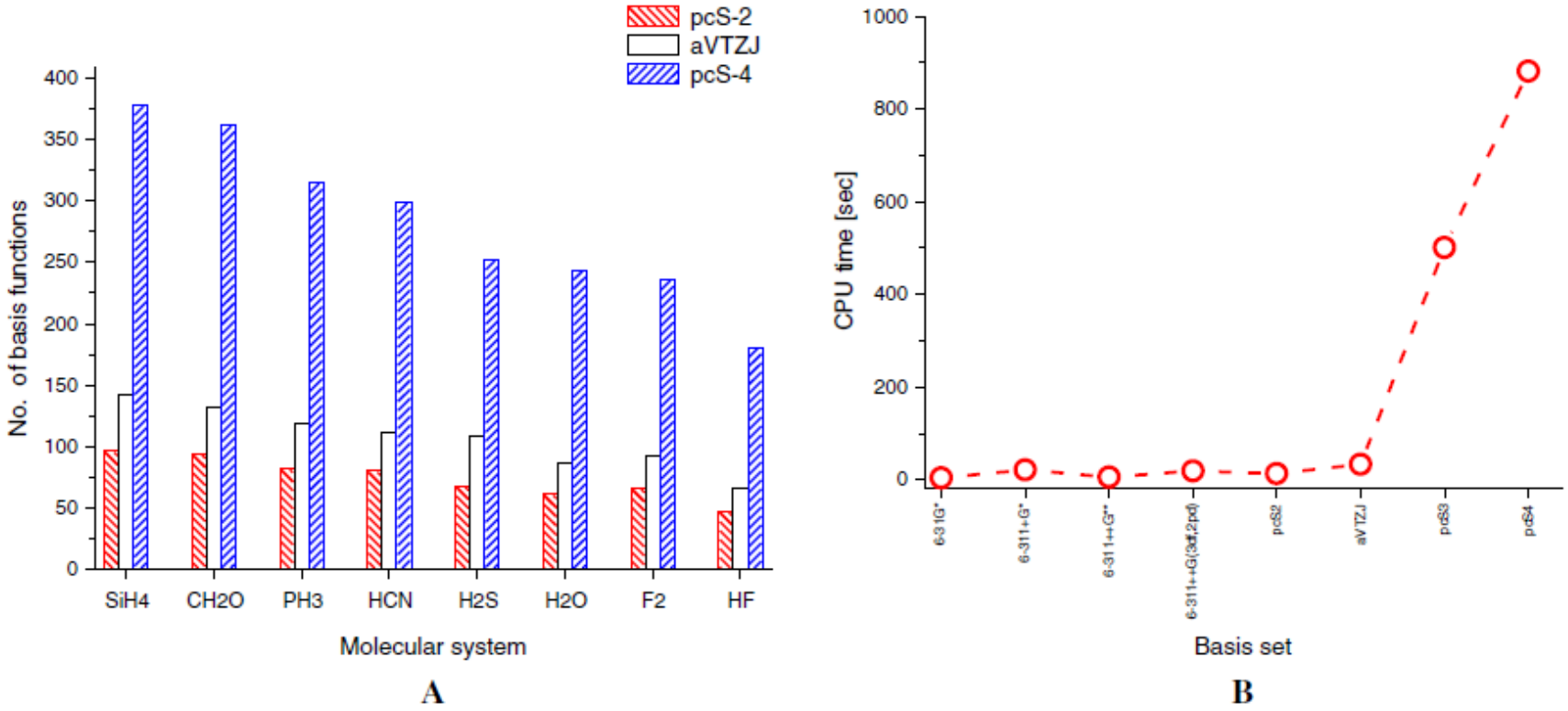


**Figure 1.** Comparison of (A) the selected basis sets size used in shielding calculations in the seven model molecules and (B) the cpu time necessary to calculate formaldehyde shieldings at the B3LYP level of theory with several basis sets.

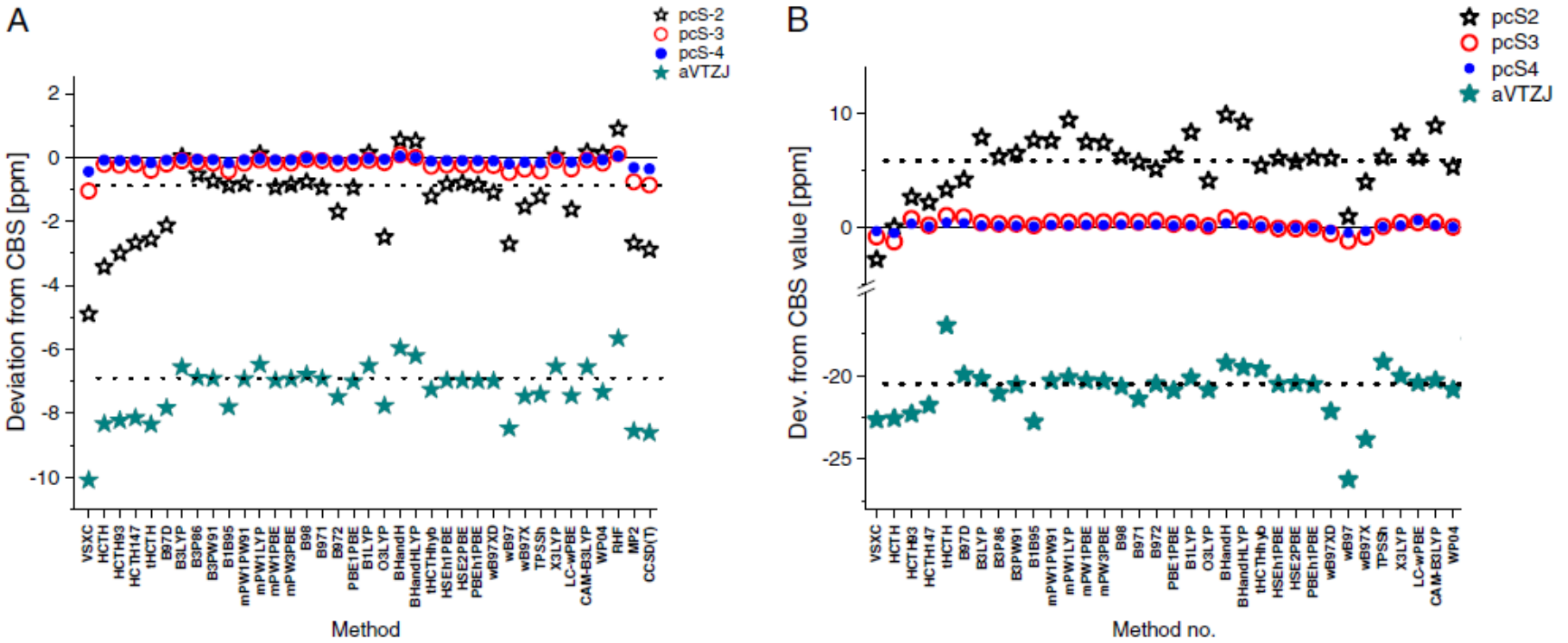


**Figure 2.** Deviations of formaldehyde (A) $^{13}C$ and (B) $^{17}O$ nuclear magnetic shieldings obtained with 37 methods and selected basis sets from the corresponding CBS values.

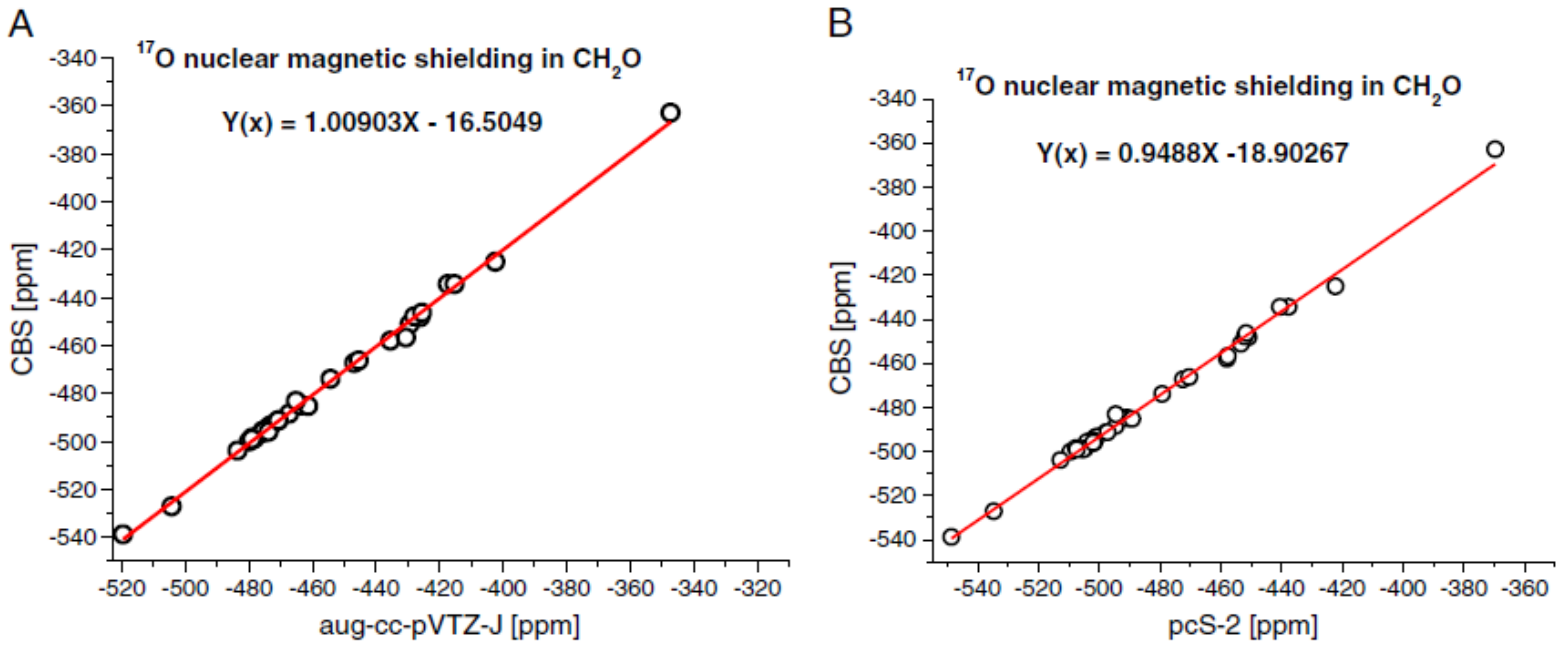


**Figure 3.** Correlations between formaldehyde $^{17}$O nuclear shieldings obtained with the 37 tested methods and with (A) aVTZJ and (B) pcS-2 basis sets *versus* the corresponding CBS (3,4) values.

**Table 3.** Deviations between empirical values of nuclear shieldings constants for nonhydrogen atom and those, calculated with B3LYP, BHandH and CCSD(T) and MP2 methods using pcS-2 and aVTZJ basis sets and the direct CBS(3,4) values as well as those, estimated from Eqns (6a) and (6b)

| | | Δ (Calc. - Emp.) | | | | |
|---|---|---|---|---|---|---|
| | | pcS2 | aVTZJ | CBS(3,4) | $CBS_2$(pcS2) | $CBS_2$(aVTZJ) |
| **C in $CH_2O$** | **B3LYP** | −34.069 | −27.486 | −34.045 | | |
| | **BHandH** | −37.222 | −30.715 | −36.675 | | |
| | **CCSD(T)** | −1.844 | 3.879 | −4.730 | −1.559 | −2.380 |
| | **MP2** | −1.893 | 3.988 | −4.572 | −1.607 | −2.272 |
| **O in $CH_2O$** | **B3LYP** | −83.180 | −55.113 | −75.301 | | |
| | **BHandH** | −128.227 | −99.134 | −118.379 | | |
| | **CCSD(T)** | 4.459 | 27.354 | 10.123 | 13.322 | 7.638 |
| | **MP2** | 50.806 | 73.255 | 57.576 | 59.669 | 53.539 |
| **O in $H_2O$** | **B3LYP** | −5.055 | −5.048 | −7.034 | | |
| | **BHandH** | 2.029 | 1.605 | −0.149 | | |
| | **CCSD(T)** | 5.606 | 5.367 | 4.057 | 3.527 | 3.497 |
| | **MP2** | 13.613 | 13.082 | 11.945 | 11.534 | 11.212 |
| **F in $F_2$** | **B3LYP** | −36.472 | −24.984 | −41.721 | | |
| | **BHandH** | −8.491 | 1.653 | −12.616 | | |
| | **CCSD(T)** | 34.430 | 42.076 | 25.748 | 29.743 | 26.573 |
| | **MP2** | 51.009 | 58.066 | 40.872 | 46.322 | 42.563 |

cd.

| | | Δ (Calc. - Emp.) | | | | |
|---|---|---|---|---|---|---|
| | | pcS2 | aVTZJ | CBS(3,4) | $CBS_2$(pcS2) | $CBS_2$(aVTZJ) |
| **F in HF** | **B3LYP** | −6.225 | −5.556 | −7.049 | | |
| | **BHandH** | −0.053 | −0.452 | −1.679 | | |
| | **CCSD(T)** | 1.762 | 1.862 | 1.458 | 0.537 | 0.502 |
| | **MP2** | 7.206 | 7.330 | 6.989 | 5.981 | 5.971 |
| **C in HCN** | **B3LYP** | −17.892 | −13.047 | −17.896 | | |
| | **BHandH** | −21.159 | −16.321 | −20.698 | | |
| | **CCSD(T)** | 0.558 | 5.583 | −0.144 | 0.786 | 0.970 |
| | **MP2** | 1.697 | 6.850 | 1.176 | 1.925 | 2.237 |
| **N in HCN** | **B3LYP** | −46.004 | −36.364 | −45.077 | | |
| | **BHandH** | −55.674 | −45.631 | −53.660 | | |
| | **CCSD(T)** | −6.062 | 2.688 | −6.122 | −4.592 | −5.683 |
| | **MP2** | 6.579 | 14.995 | 6.406 | 8.049 | 6.624 |
| **S in $H_2S$** | **B3LYP** | −45.365 | −43.310 | −44.073 | | |
| | **BHandH** | −12.824 | −11.357 | −12.082 | | |
| | **CCSD(T)** | −6.193 | 0.265 | 1.126 | −5.176 | −0.479 |
| | **MP2** | 11.063 | −26.869 | 17.838 | 12.080 | −27.613 |
| **Si in $SiH_4$** | **B3LYP** | −53.474 | −41.496 | −54.554 | | |
| | **BHandH** | −39.711 | −28.903 | −41.719 | | |
| | **CCSD(T)** | −22.154 | −16.325 | −21.120 | −23.698 | −29.262 |
| | **MP2** | −12.557 | −5.036 | −15.500 | −14.101 | −17.973 |

Research Article

Magnetic Resonance in Chemistry

Received: 15 March 2013 Revised: 16 April 2013 Accepted: 1 May 2013 Published online in Wiley Online Library: 5 June 2013

(wileyonlinelibrary.com) DOI 10.1002/mrc.3972

# $^3$He NMR: from free gas to its encapsulation in fullerene

Teobald Kupka,[a]* Michał Stachów,[a,b] Leszek Stobiński[c] and Jakub Kaminský[d]

**The $^3$He nuclear magnetic shieldings were calculated for single helium atom, its dimer, simple models of fullerene cages (He@$C_n$), and single wall carbon nanotubes. The performances of several levels of theory (HF, MP2, DFT-VSXC, CCSD, CCSD(T), and CCSDT) were tested. Two sets of polarization-consistent basis sets were used (pcS-n and aug-pcS-n), and an estimate of $^3$He nuclear magnetic shieldings in the complete basis set limit using a two-parameter fit was established. Theoretical $^3$He results reproduced accurately previously reported theoretical values for helium gas, dimer, and helium probe inside several fullerene cages. Excellent agreement with experimental values was achieved. $^3$He nuclear magnetic shieldings of single helium atom approaching various points of benzene ring were tested, and an impact of $^3$He confinement within fullerene cages of different size on the $^3$He chemical shift was determined. Copyright © 2013 John Wiley & Sons, Ltd.**

**Keywords:** $^3$He NMR; GIAO; molecular modeling; ab initio; fullerene; SWCNT

**Table 1.** Calculated $^{3}$He isotropic shielding constant [ppm] for helium single atom and $He_2$ using RHF, MP2, VSXC and coupled cluster methods combined with selected Jensen's basis sets (pcS-n and aug-pcS-n)

| Method | Basis set | | | | | | | | Literature |
|---|---|---|---|---|---|---|---|---|---|
| | pcS-2 | pcS-3 | pcS-4 | CBS | aug-pcS-2 | a-pcS-3 | a-pcS-4 | CBS | |
| | | | | He | | | | | |
| HF | 59.881 | 59.899 | 59.900 | 59.900 | 59.889 | 59.899 | 59.900 | 59.900 | 59.892[a] |
| MP2 | 59.919 | 59.963 | 59.964 | 59.964 | 59.912 | 59.960 | 59.963 | 59.964 | 59.967[b] |
| VSXC | 60.092 | 60.111 | 60.112 | 60.112 | 60.070 | 60.112 | 60.112 | 60.112 | 59.908038[c] |
| CCSD | 59.892 | 59.921 | 59.927 | 59.930 | 59.886 | 59.920 | 59.926 | 59.930 | |
| | | | | $He_2$ | | | | | |
| HF | 59.881 | 59.899 | 59.901 | 59.902 | 59.890 | 59.899 | 59.900 | 59.900 | 59.906277[c] |
| MP2 | 59.920 | 59.962 | 59.963 | 59.963 | 59.910 | 59.960 | 59.962 | 59.963 | |
| VSXC | 60.087 | 60.103 | 60.103 | 60.103 | 60.058 | 60.102 | 60.101 | 60.101 | |
| CCSD | 59.892 | 59.920 | 59.925 | 59.927 | 59.884 | 59.918 | 59.925 | 59.926 | |
| CCSD(T) | 59.892 | 59.920 | 59.925 | | 59.884 | 59.918 | 59.924 | | |
| CCSDT | 59.892 | 59.920 | 59.925 | | 59.883 | 59.918 | 59.924 | | |

[a]from comparison with $^{1}$H resonance frequency from reference.[29]
[b]relativistic value including a number of smaller effects from reference.[80]
[c]exact result taken from reference.[46]

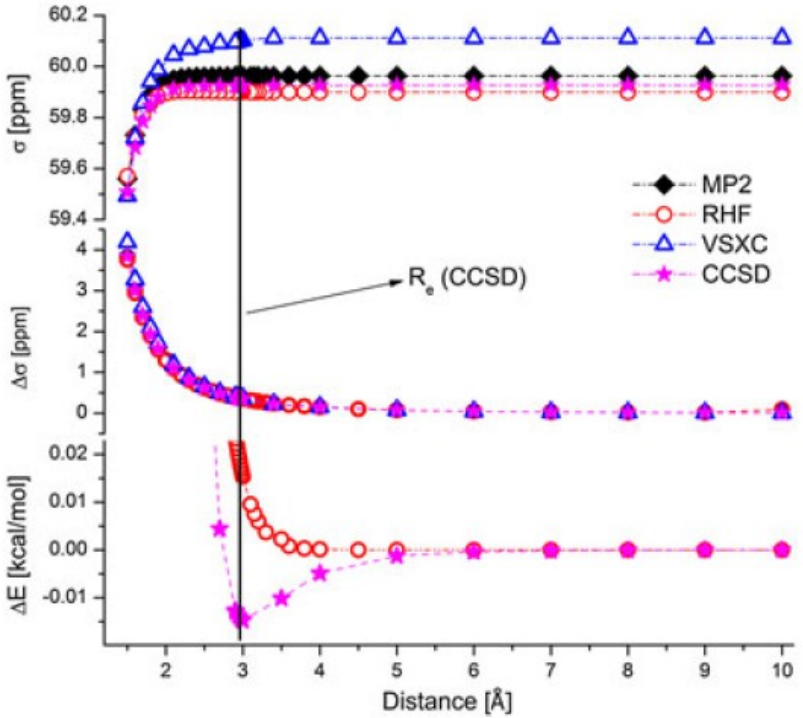


**Figure 2.** Change of $^3$He isotropic shielding constant ($\sigma$ in ppm) and shielding anisotropy ($\Delta\sigma$ in ppm) upon $He_2$ formation by using RHF, MP2 and VSXC and CCSD methods and aug-pcS-4 basis set (only pcS-4 basis set used for CCSD). The corresponding dimerization energy ($\Delta E$ in kcal/mol) is also shown for CCSD and RHF calculations. For the reader's convenience, the individual points are connected.

**Table 2.** Calculated $^3$He isotropic shielding constant and anisotropy [ppm] for helium dimer at experimental $R_e = 2.97$ Å using RHF, MP2, VSXC, and CCSD methods. Jensen's aug-pcS-4 (RHF, MP2 and VSXC) and pcS-4 (for CCSD) basis sets were applied

| Method | Shielding | Anisotropy |
|---|---|---|
| RHF | 59.901 | 0.359 |
| MP2 | 59.962 | 0.360 |
| VSXC | 60.101 | 0.374 |
| CCSD | 59.925 | 0.362 |

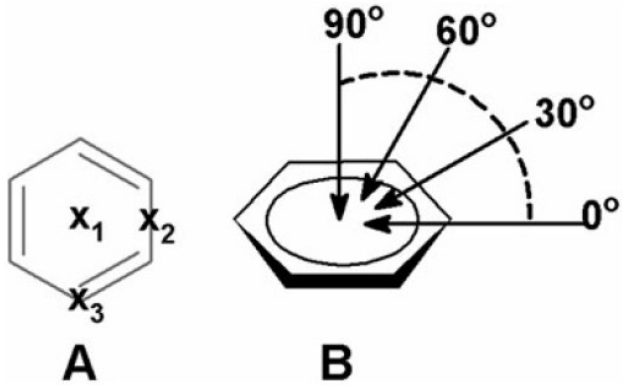


**Figure 1.** (A) Schematic positions of helium atom approaching a benzene ring marked by *x*. (B) He atom approaching a selected point in benzene ring at several angles to ring plane.

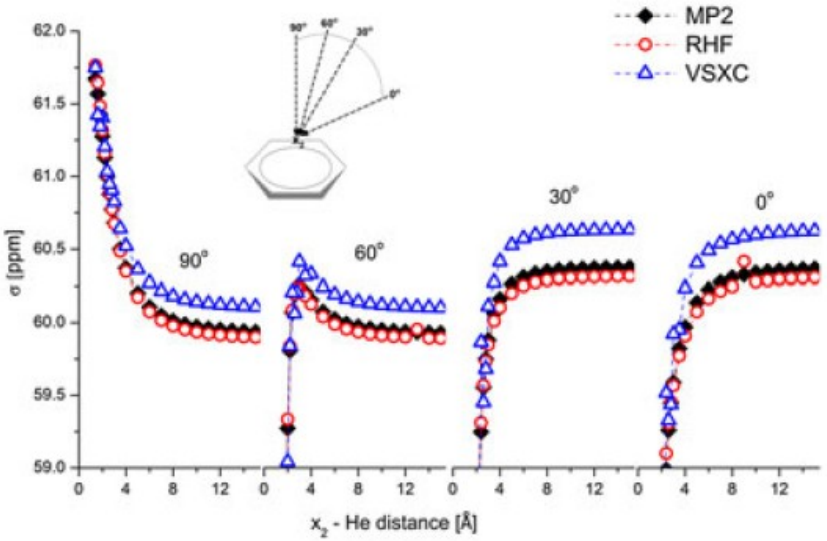


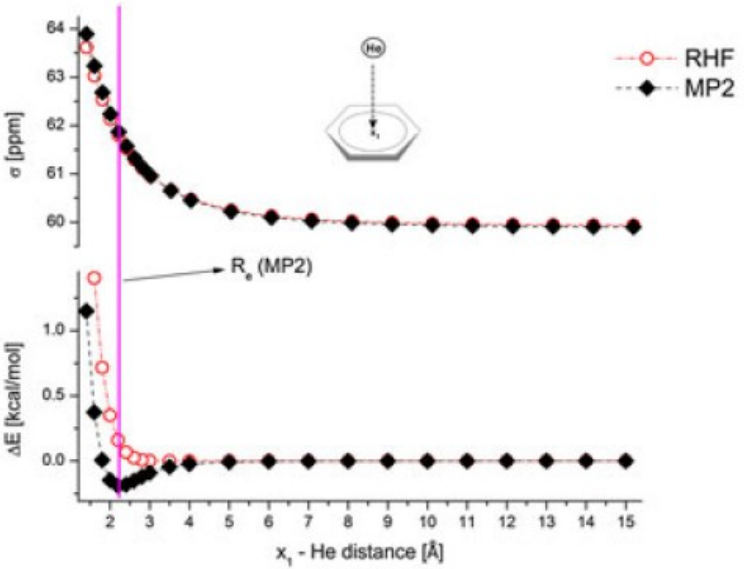


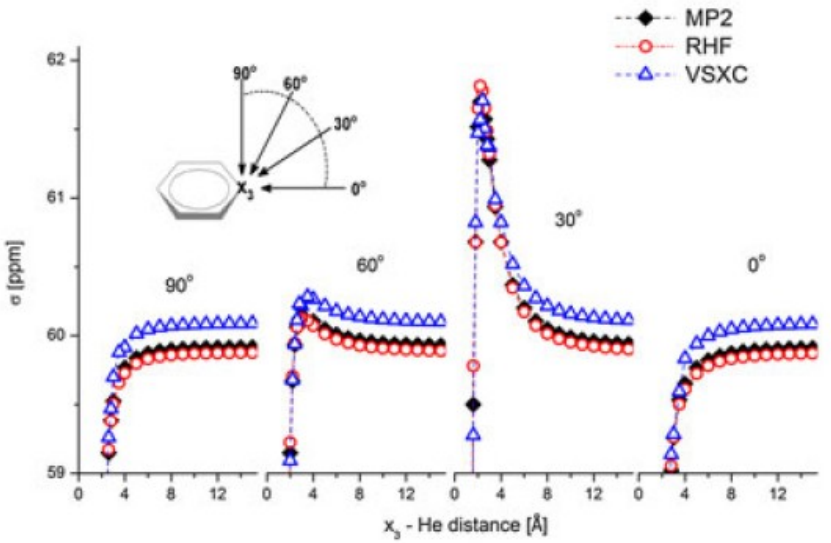


**Figure 3.** Change of $^{3}$He NMR isotropic shielding constant and binding energy (ΔE in kcal/mol), calculated with RHF, MP2, and VSXC methods and pcS-2 basis set upon helium atom approaching (top) the middle of benzene ring, (middle) the middle of C=C bond and (bottom) carbon atom (He trajectory depicted in Fig. 1). For the reader's convenience, individual points are connected.

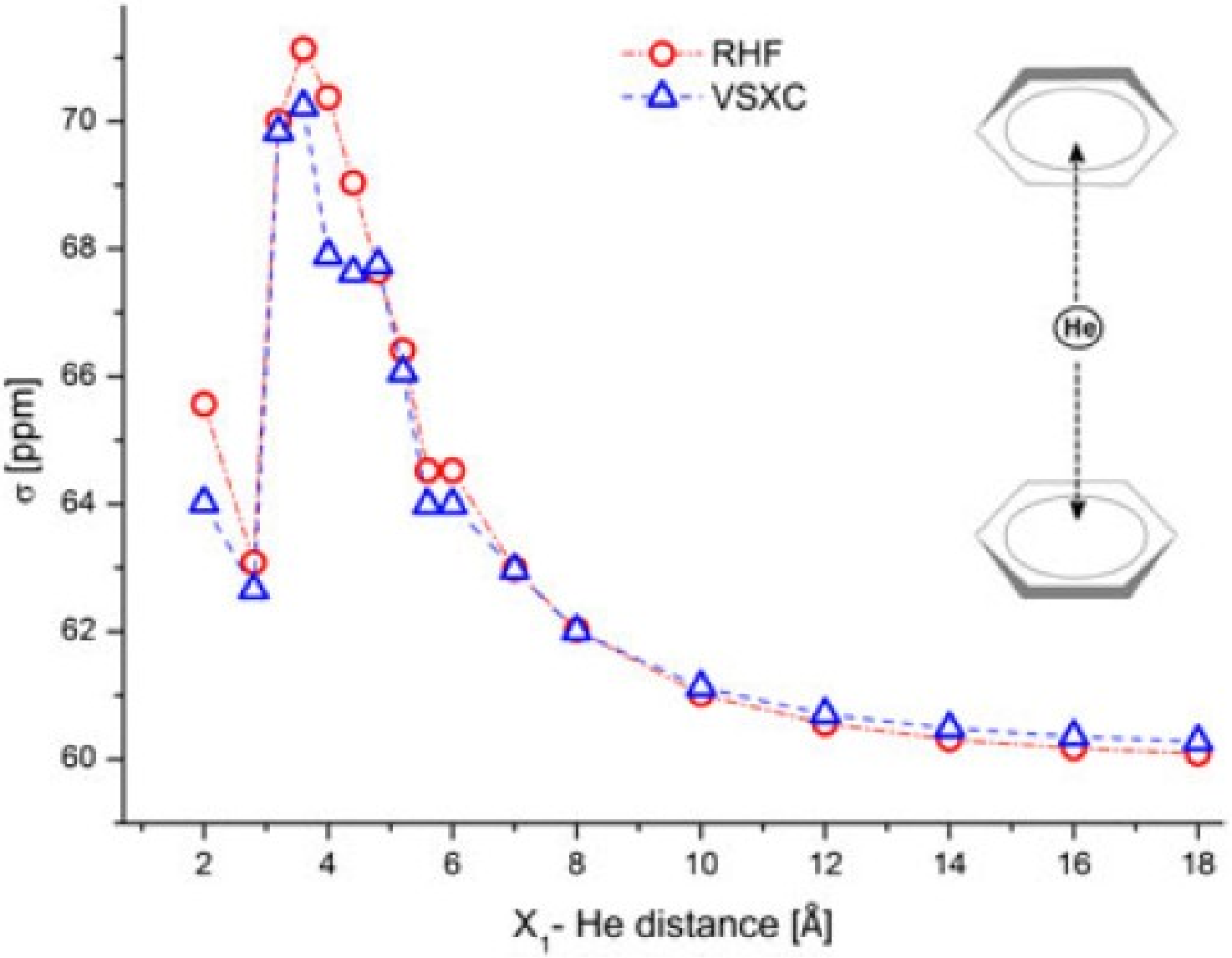


**Figure 4.** Change of $^{3}$He NMR isotropic shielding constant calculated with RHF and VSXC methods and pcS-2 basis set upon helium atom between the middle of two moving benzene rings. For the reader's convenience, individual points are connected.

**Table 3.** Comparison of calculated $^{3}$He NMR chemical shift δ (in ppm) for selected fullerenes using VSXC method and pcS-2 Jensen's basis set with available literature values and experiment

| System | δ [ppm] | | | |
|---|---|---|---|---|
| | This work | DFT[a] | HF[a] | Exp.[a] |
| $He@C_{32}(C_2)$ | −26.20 | | | |
| $He@C_{32}(D_2)$ | −0.67 | | | |
| $He@C_{34}(C_2)$ | −1.28 | | | |
| $He@C_{60}(I_h)$ | −5.219 | −1.46 | −10.86 | −6.40 |
| $He@C_{70}(D_{5h})$ | −23.29 | −29.86 | −30.14 | −28.82 |
| $He@C_{76}(D_2)$ | −16.57 | −16.85 | −21.43 | −18.75 |

[a]from reference.[27]

JCTC Journal of Chemical Theory and Computation

Article

pubs.acs.org/JCTC

# Efficient Modeling of NMR Parameters in Carbon Nanosystems

Teobald Kupka,*[,†] Michał Stachów,[†] Elżbieta Chełmecka,[§] Karol Pasterny,[∥] Magdalena Stobińska,[⊥,#] Leszek Stobiński,[▽] and Jakub Kaminský[○]

[†]University of Opole, Faculty of Chemistry, 48, Oleska Street, 45-052 Opole, Poland

[§]Division of Statistics, Department of Instrumental Analysis, Medical University of Silesia, 30 Ostrogórska Street, 41-200 Sosnowiec, Poland

[∥]A. Chełkowski Institute of Physics, University of Silesia, 4 Uniwersytecka Street, 40-007 Katowice, Poland

[⊥]Institute of Theoretical Physics and Astrophysics, University of Gdańsk, 57 Wita Stwosza Street, 80-952 Gdańsk, Poland

[#]Institute of Physics, Polish Academy of Sciences, 32/46, al. Lotników, 02-668 Warsaw, Poland

[▽]Institute of Physical Chemistry, Polish Academy of Sciences, 44/52 Kasprzaka Street, 01-224 Warsaw, Poland

[○]Institute of Organic Chemistry and Biochemistry, Czech Academy of Sciences, Flemingovo Nam. 2., 166 10 Prague, Czech Republic

*Supporting Information*

**ABSTRACT:** Rapid growth of nanoscience and nanotechnology requires new and more powerful modeling tools. Efficient theoretical modeling of large molecular systems at the *ab initio* and Density Functional Theory (DFT) levels of theory depends critically on the size and completeness of the basis set used. The recently designed variants of STO-3G basis set (STO-3G$_{el}$, STO-3G$_{mag}$), modified to correctly predict electronic and magnetic properties were tested on simple models of pristine and functionalized carbon nanotube (CNT) systems and fullerenes using the B3LYP and VSXC density functionals. Predicted geometries, vibrational properties, and HOMO/LUMO gaps of the model systems, calculated with typical 6-31G* and modified STO-3G basis sets, were comparable. The $^{13}$C nuclear isotropic shieldings, calculated with STO-3G$_{mag}$ and Jensen's polarization consistent pcS-2 basis sets, were also identical. The STO-3G$_{mag}$ basis sets, being half the size of the latter one, are promising alternative for studying $^{13}$C nuclear magnetic shieldings in larger size CNTs and fullerenes.

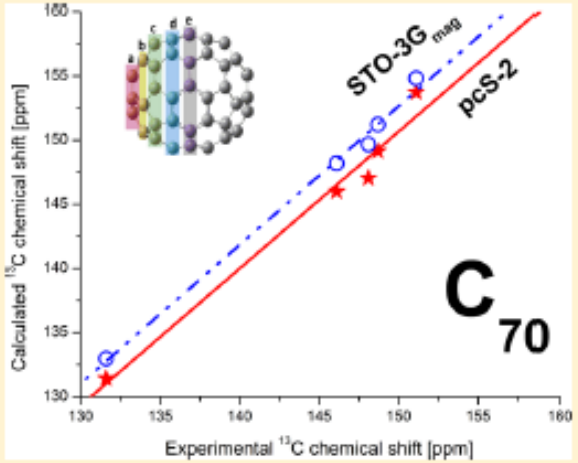

**Scheme 1. Bond Labeling in Linearly Conjugated Planar (p) Benzene Rings (acenes, $n$ = 1–9)**

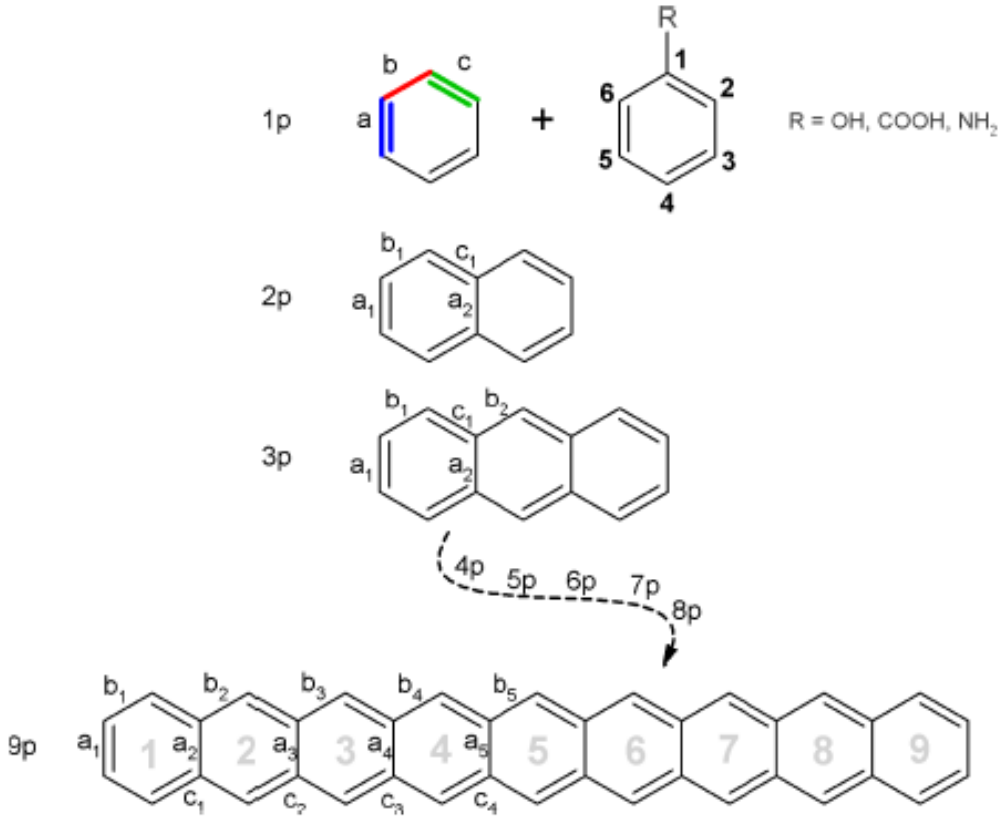


**Scheme 2. Bond Labeling in Molecular "Belt" Systems (Cyclacenes, where $n$ = 4–8)**

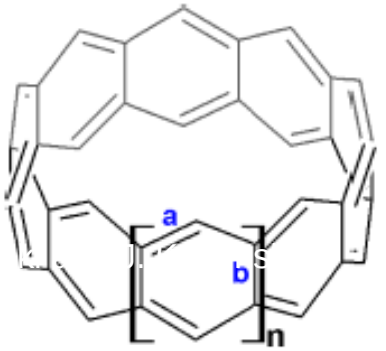

Scheme 3. Bond and Atom Labeling in Short *Zigzag* (4,0) SWCNT Model Consisting of Five "Bamboo" Units[a]

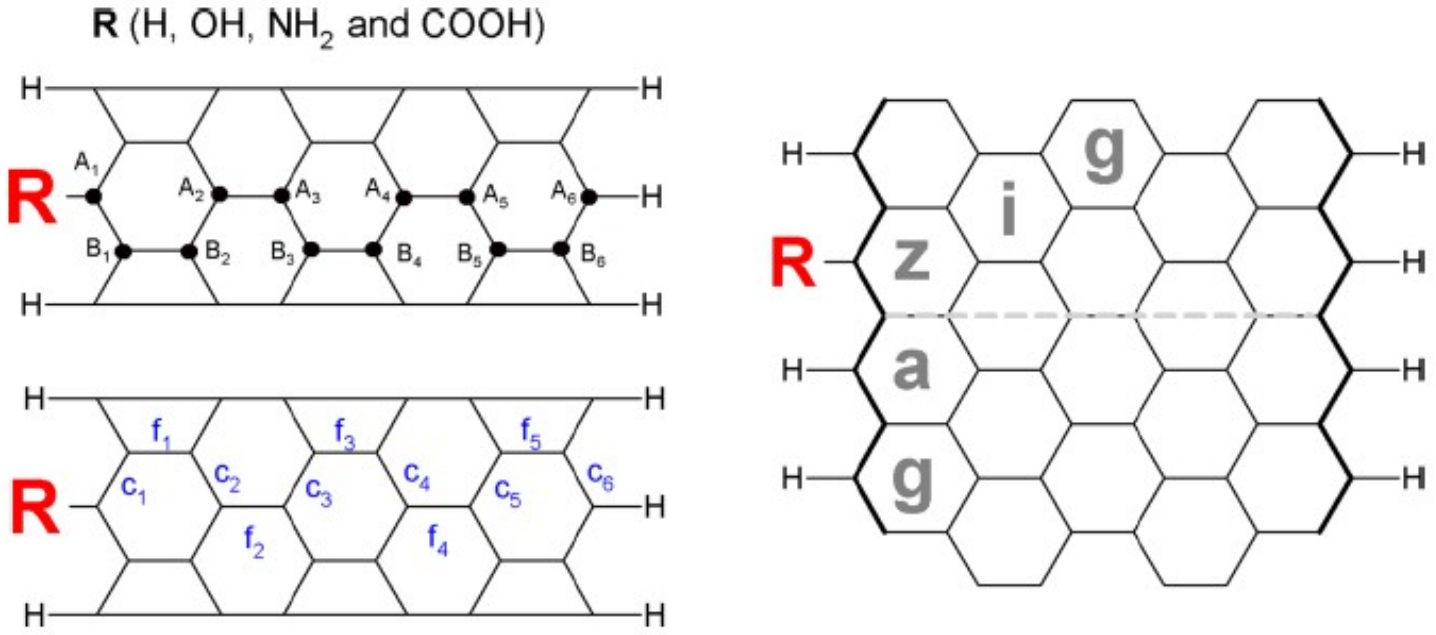


[a]A dashed line indicates tube axis and the two *zigzag* type rims are marked by a thicker line.

**Table 1. Performance[a,b] of STO-3G$_{el}$ and STO-3G$_{mag}$ Basis Sets in Predicting Deviations of Bond Lengths (in Å) and Selected IR/Raman Vibrations (in cm$^{-1}$) from Experimental Values of Benzene, Phenol, Aniline, and Benzoic Acid**

| | basis set | | | | |
|---|---|---|---|---|---|
| method | STO-3G | 6-31G* | STO-3G$_{el}$ | STO-3G$_{mag}$ | pcS-2 |
| | | | Bond Length | | |
| B3LYP | 0.0269 | 0.0051 | 0.0043 | 0.0075 | 0.0091 |
| VSXC | 0.0298 | 0.0111 | 0.0039 | 0.0086 | 0.0055 |
| | | | Harmonic Vibration | | |
| B3LYP | 265.73 | 111.79 | 91.29 | 146.27 | 124.85 |
| VSXC | 248.21 | 95.25 | 92.05 | 124.34 | 114.85 |

[a]RMS values from experimental values are given. [b]Results obtained with selected basis sets are given for comparison.

## Table 3. CPU Time (min) of Benzene Calculations

| | | CPU Time | | |
|---|---|---|---|---|
| basis set | N | opt. | freq. | NMR |
| | | B3LYP (VSXC) | | |
| STO-3G | 36 | 3.8 (7.2) | 8.9 (10.4) | 1.1 (2.3) |
| 6-31G* | 102 | 7.6 (16.8) | 33.5 (55.4) | 5.2 (5.7) |
| STO-3G$_{el}$ | 126 | 6.6 (37.5) | 80.2 (132.5) | 9.2 (11.2) |
| STO-G$_{mag}$ | 126 | 7.3 (36.3) | 70.0 (125.5) | 7.9 (14.2) |
| pcS-2 | 282 | 29.5 (69.9) | 190.3 (301.9) | 50.2 (44.1) |

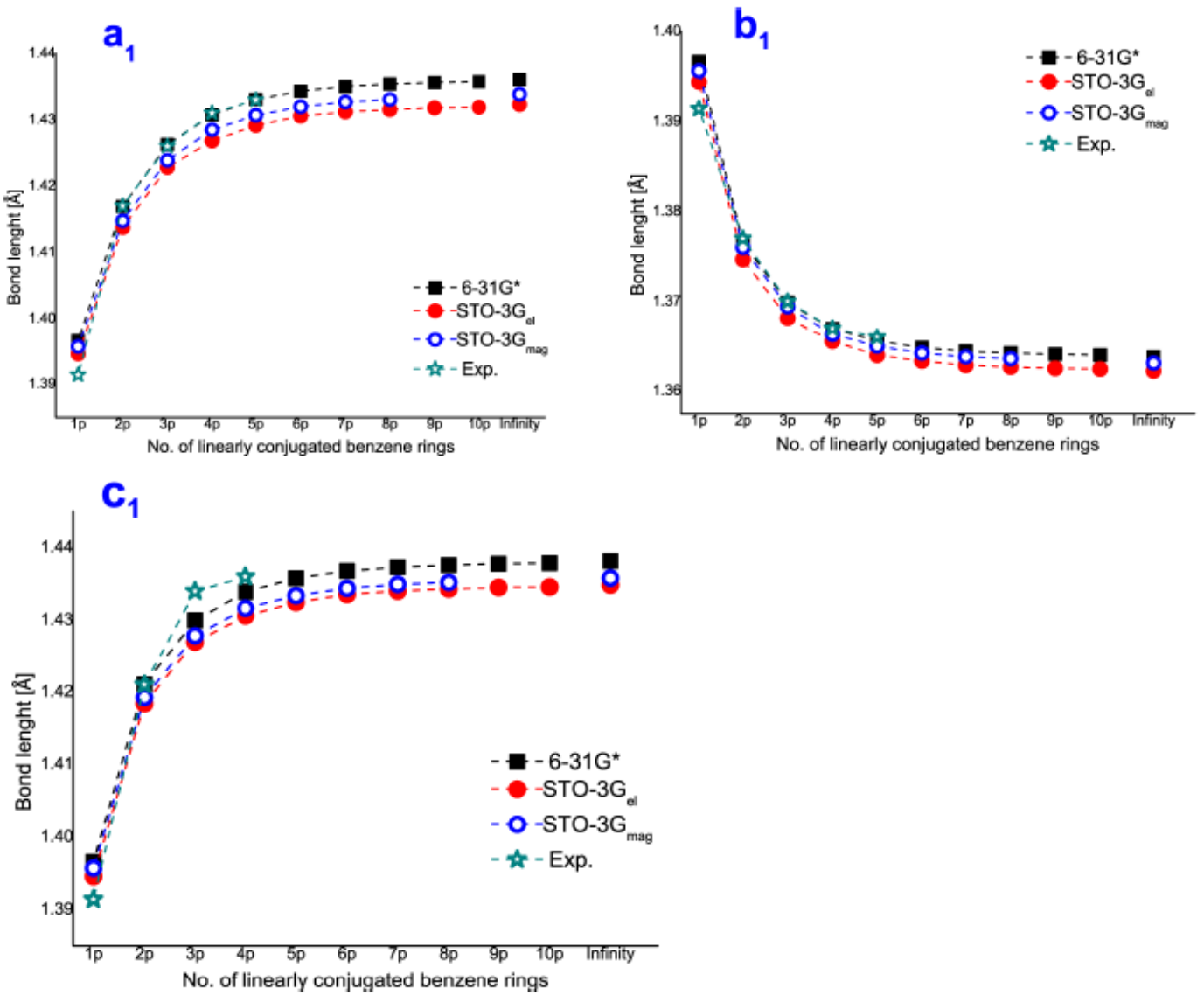


Figure 1. Regular convergence of three types of C−C bond lengths in polyaromatic hydrocarbons, calculated using B3LYP combined with 6-31G*, STO-3G$_{mag}$, and STO-3G$_{el}$ basis sets, upon increasing the number of linearly conjugated benzene rings (see Scheme 1): (A) $a_1$ type, (B) $b_1$ type, (C) $c_1$ type. Experimental data are from refs 78, 101−103 and individual points are connected for the reader's convenience.

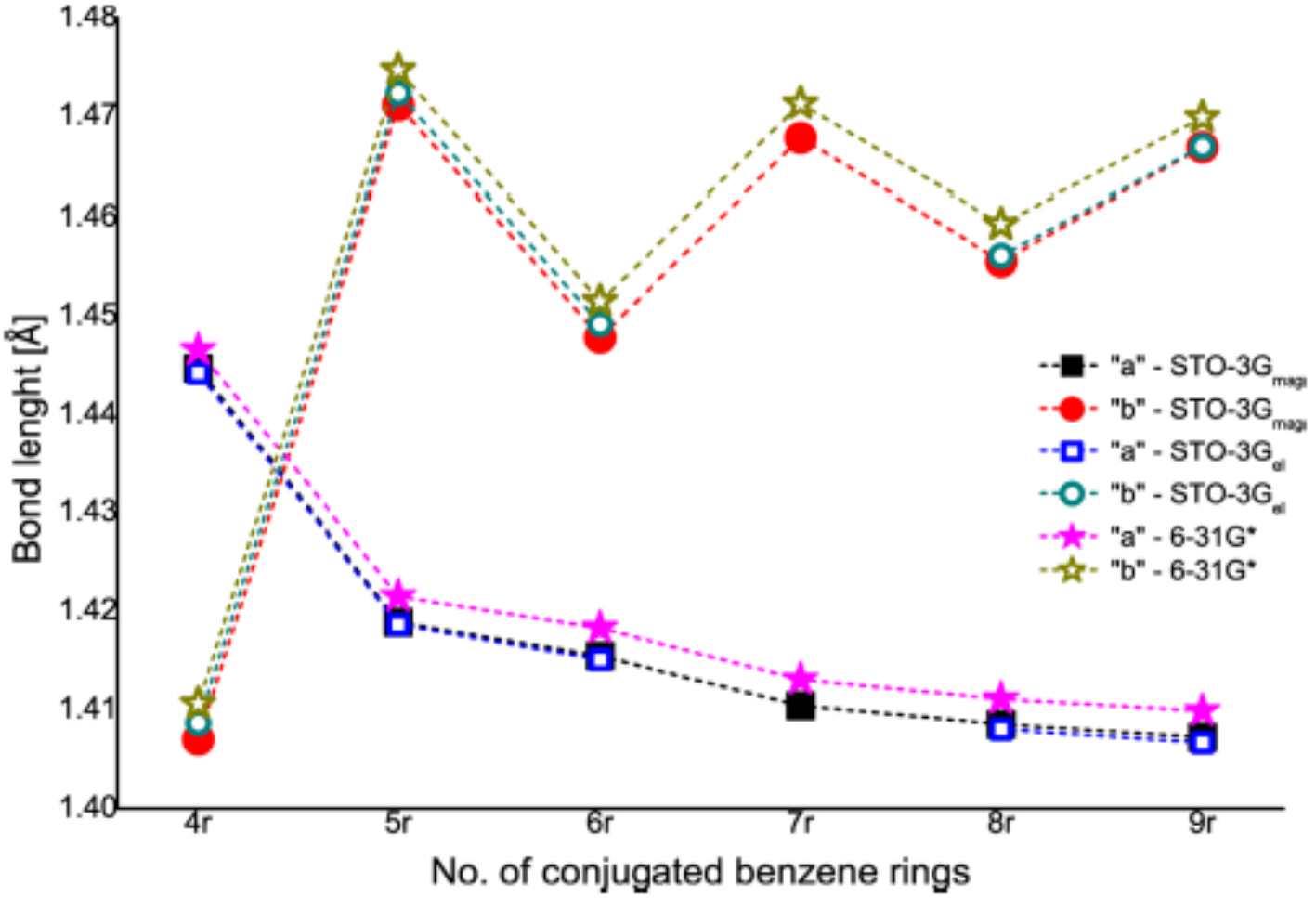


Figure 2. Convergence of two different types of C–C bond lengths (*a* and *b*, see Scheme 2) in cyclacenes calculated using B3LYP density functional combined with 6-31G*, STO-3$G_{mag}$, and STO-3$G_{el}$ basis sets upon increasing the number of benzene rings. In some cases, very similar results obtained with different basis set are indicated by overlapping marks. Individual points are connected for the reader's convenience.

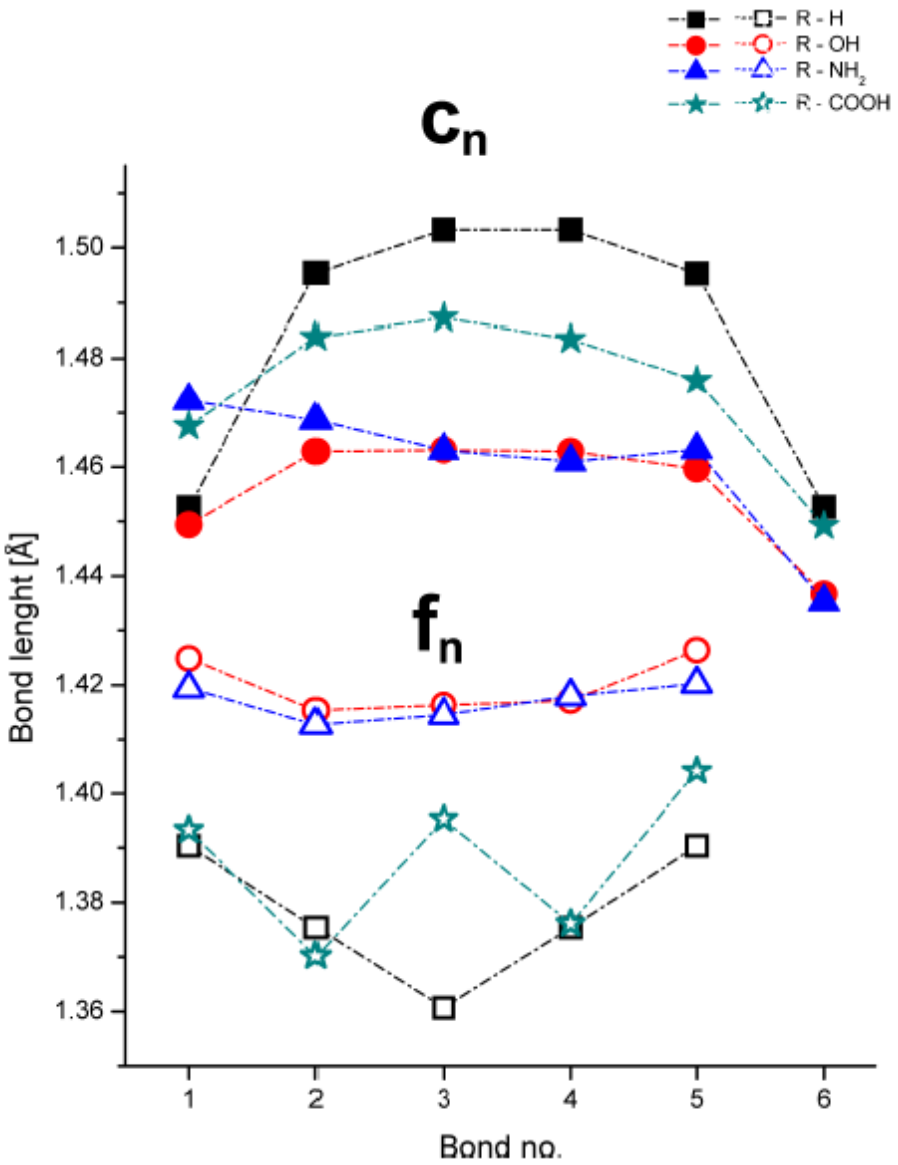


Figure 3. Influence of the tip-substituent nature on (A) $c_1$ to $c_6$ and (B) $f_1$ to $f_5$ type of C–C bond length along the axis of a model *zigzag* (4,0) SWCNT. The bond-lengths were calculated at the B3LYP/6-31G** level. In some cases, very similar results obtained for different functionalization are indicated by overlapping marks. For reader's convenience the individual points are connected.

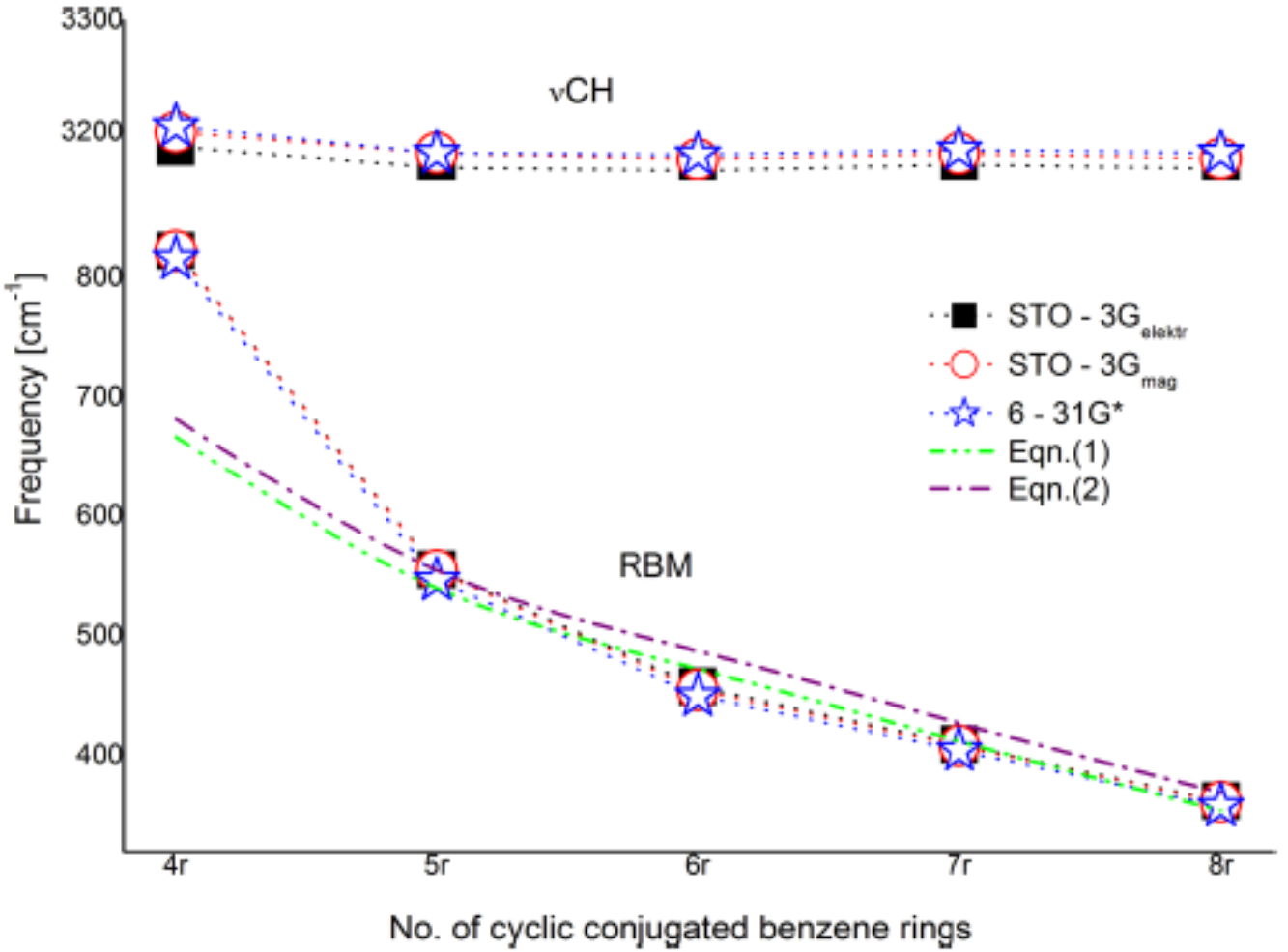


**Figure 4.** Convergence of RBM and $\nu$(CH) wavelengths in cyclacenes upon increasing the number of benzene rings, calculated using B3LYP density functional combined with 6-31G*, STO-3G$_{mag}$, and STO-3G$_{el}$ basis sets. In some cases, very similar results obtained with different basis set are indicated by overlapping marks. Empirical results for SWCNTs calculated with eq 1 and 2 are shown for comparison. Individual points are connected for the reader's convenience.

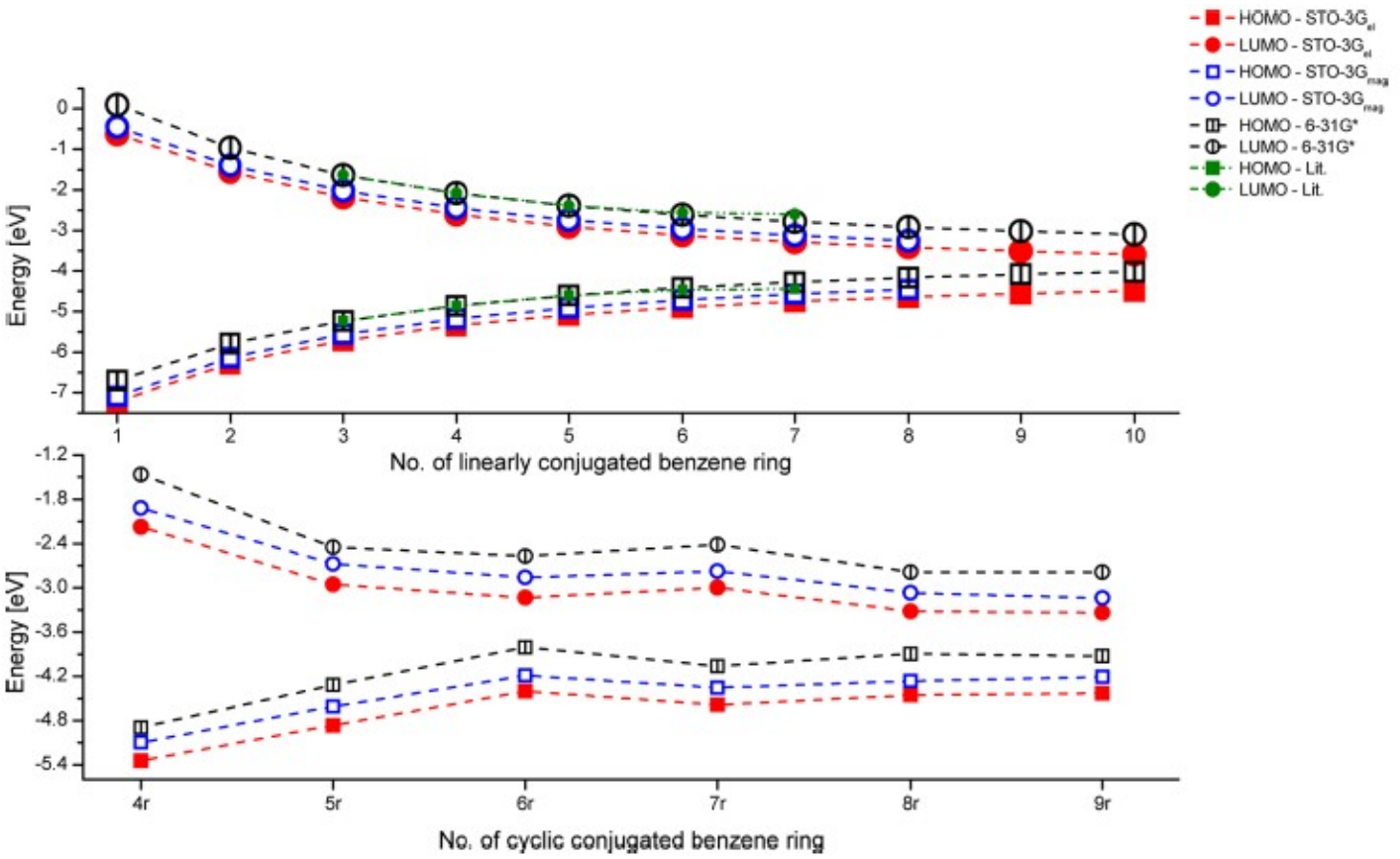


Figure 5. B3LYP calculated HOMO and LUMO molecular orbital energies [eV] in polyacenes (top) and cyclacenes (bottom) as a function of the number of benzene rings ($n$). In some cases, very similar results obtained with different basis set are indicated by overlapping marks. Individual points are connected for the reader's convenience.

**Table 4. B3LYP Calculated HOMO−LUMO Gap [eV] for Linear acenes, Cyclacenes, and *Zigzag* (4,0) SWCNT Containing 5 "Bamboo" Units**

| | HOMO−LUMO gap [eV] | | | | |
|---|---|---|---|---|---|
| | basis set | | | | |
| molecular system | 6-31G* | STO-3G$_{el}$ | STO-3G$_{mag}$ | lit. | exp. |
| | Polyacene | | | | |
| 1p | 6.8[a] | 6.59[e] | 6.64[e] | | 5.96[f] |
| 2p | 4.83[a] | 4.73[e] | 4.74[e] | | 4.45[g] |
| 3p | 3.59[a] | 3.53[e] | 3.53[e] | 3.59[b] | 3.45[g] |
| 4p | 2.78[a] | 2.73[e] | 2.73[e] | 2.78[b] | 2.72[g] |
| 5p | 2.21[a] | 2.17[e] | 2.16[e] | 2.21[b] | 2.31[g] |
| | | | | | 2.29[g] |
| 6p | 1.8[a] | 1.77[e] | 1.75[e] | 1.89[b] | 1.90[g] |
| 7p | 1.49[a] | 1.46[e] | 1.44[e] | 1.86[b] | 1.35[h] |
| 8p | 1.25[a] | 1.23[e] | 1.20[e] | | |
| 9p | 1.06[a] | 1.05[e] | | | |
| infinity | 0.91[a] | | | 1.61 | ≈1.2[i] |
| infinity[c] | 0.77[a] | 1.11[e] | 1.28[e] | 1.86[e] | 1.55[e] |
| | Cyclacene | | | | |
| 4r | 3.43[a] | 3.17[e] | 3.18[e] | | |
| 5r | 1.87[a] | 1.91[e] | 1.93[e] | | |
| 6r | 1.24[a] | 1.27[e] | 1.33[e] | | |
| 7r | 1.65[a] | 1.59[e] | 1.58[e] | | |
| 8r | 1.11[a] | 1.14[e] | 1.20[e] | | |
| infinity[d] | 1.09[a] | 1.36[e] | 1.38[e] | | |
| pristine (4,0) SWCNT (4r5u) | | | | 1.05[e] | |
| (4,0) HO-SWCNT (4r5u) | | | | 1.08[e] | |
| (4,0) $H_2N$-SWCNT (4r5u) | | | | 1.09[e] | |
| (4,0) HOOC-SWCNT (4r5u) | | | | 1.09[e] | |
| $C_{60}(I_h)$ | | | | 2.89[e] | 2.3[j] |
| $C_{70}(D_{5h})$ | | | | 2.69[e] | |
| $C_{76}(D_2)$ | | | | 1.97[e] | |

[a]From ref 67. [b]From ref 109. [c]CBS fit with eq 3. [d]Data for 7r excluded from fitting with eq 4. [e]This work. [f]From ref 111. [g]From ref 115. [h]Simplest measured derivative from ref 116. [i]Extrapolated value from ref 116. [j]From ref 112. Data obtained from extrapolation to infinite size systems are also included.

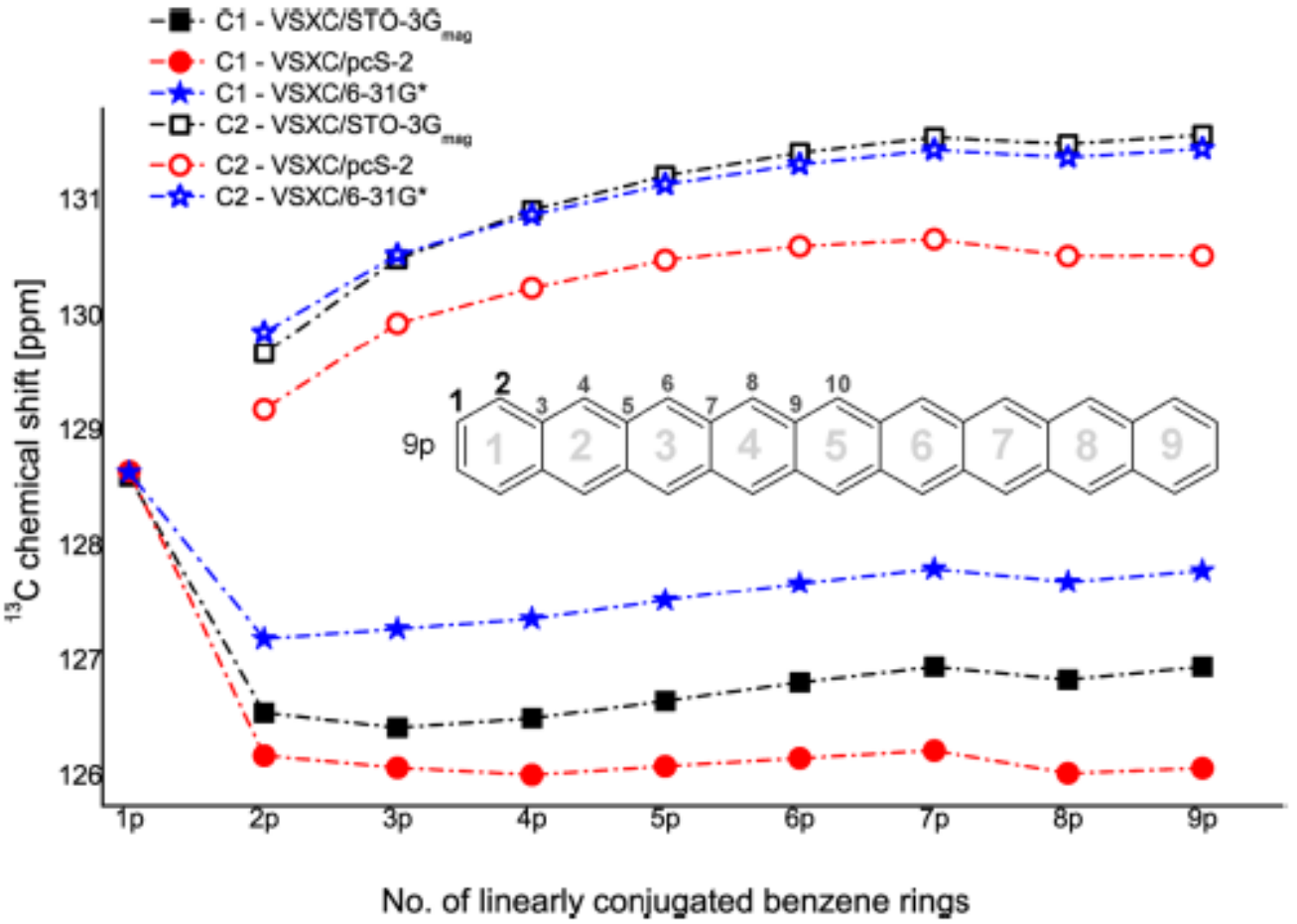


Figure 6. Different convergence of $^{13}$C chemical shifts of two carbons (B3LYP/6-31G* geometry, C1 full marks, C2 empty marks) in polyaromatic hydrocarbons calculated with VSXC density functional combined with 6-31G*, STO-3G$_{mag}$, and pcS-2 basis sets, upon increasing the number of linearly conjugated benzene rings (see Scheme 1). In some cases, very similar results obtained with different basis set are indicated by overlapping marks. Individual points are connected for the reader's convenience.

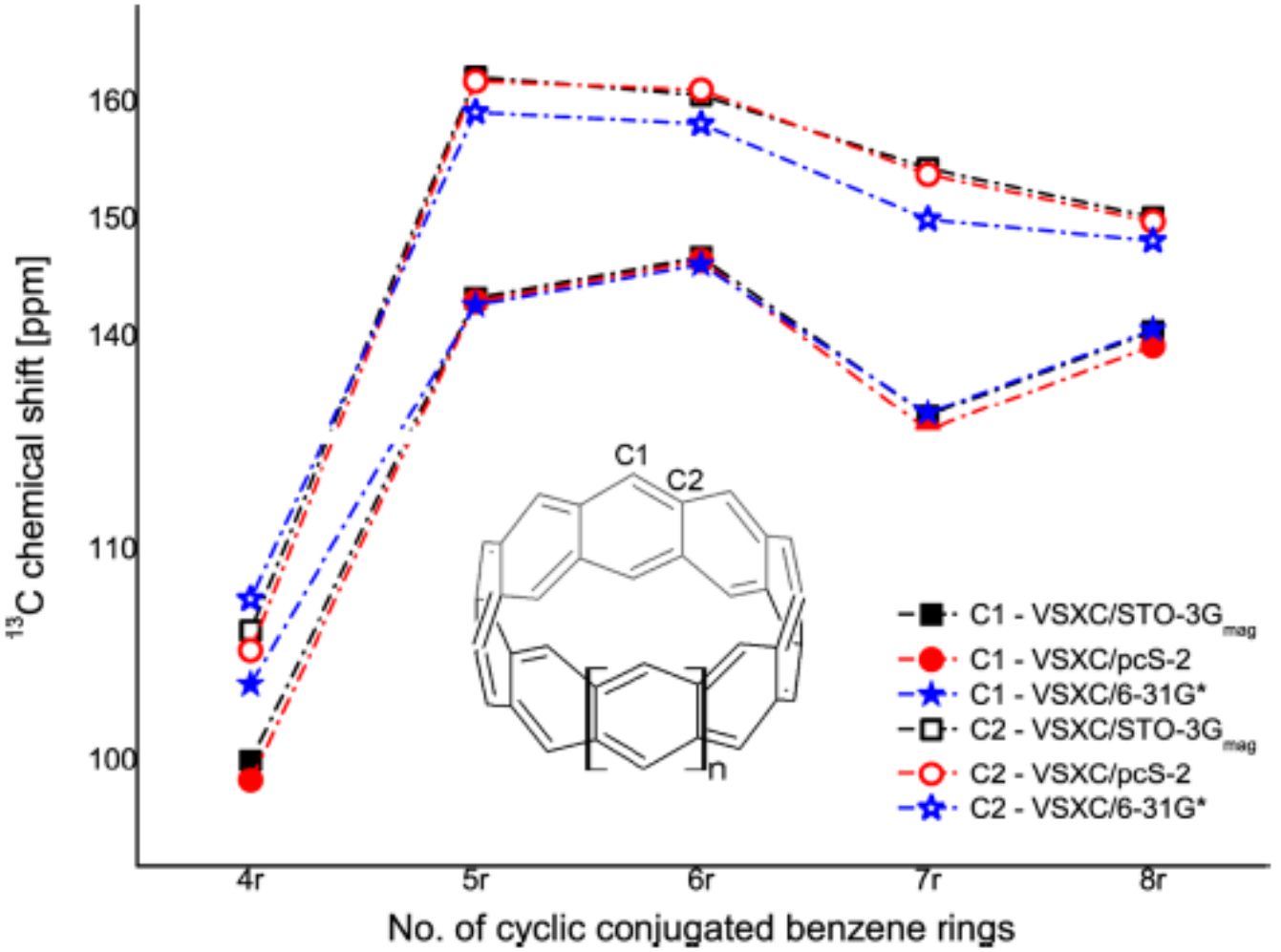


Figure 7. Different convergence of two types of $^{13}$C chemical shifts in polyaromatic hydrocarbons (B3LYP/6-31G* geometry) calculated using VSXC density functional combined with 6-31G*, STO-3G$_{mag}$, and STO-3G$_{el}$ basis sets, upon increasing the number of benzene rings in cyclacenes (see Scheme 2). In some cases, very similar results obtained with different basis sets are indicated by overlapping marks. Individual points are connected for the reader's convenience.

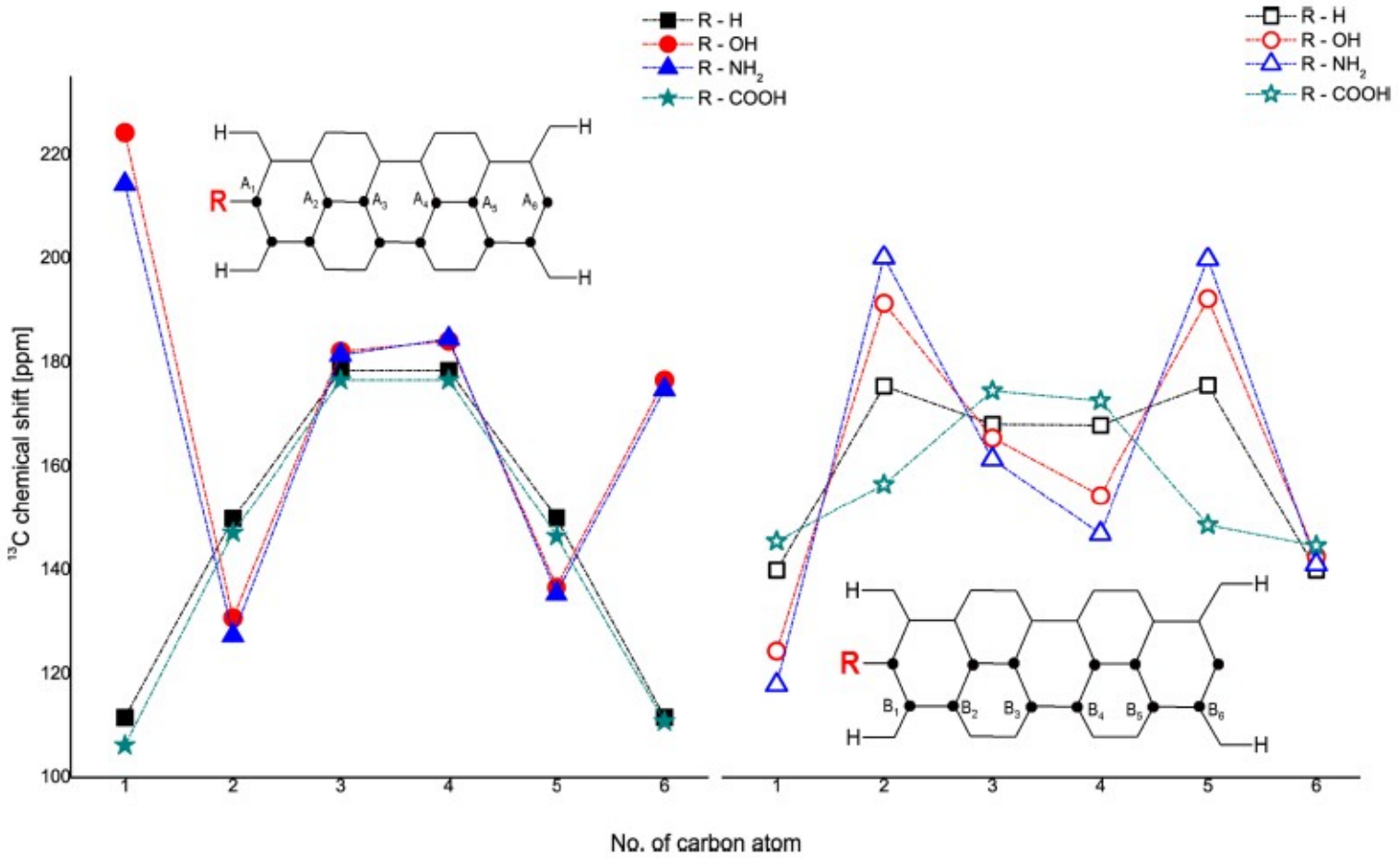


Figure 8. Different convergence of (A) A1 to A6 and (B) B1 to B6 types of $^{13}C$ chemical shifts in short functionalized *zigzag* (4,0) SWCNT along the tube axis (see Scheme 3). Structures were optimized with B3LYP/6-31G* method, and shifts were calculated using the VSXC density functional combined with STO-3$G_{mag}$ basis set. In some cases, very similar results obtained for different systems are indicated by overlapping marks. Individual points are connected for the reader's convenience.

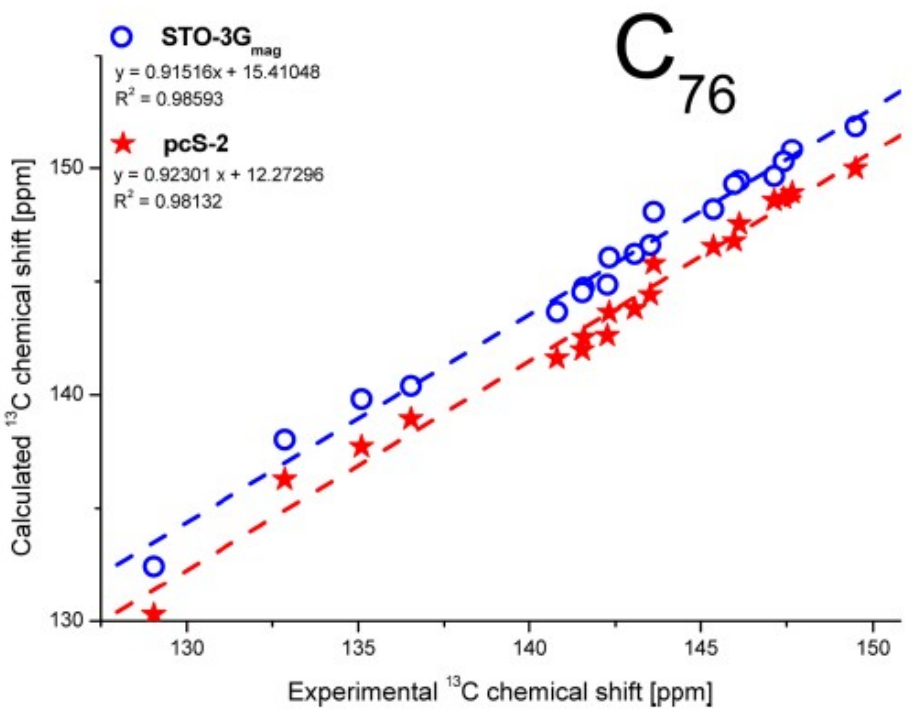


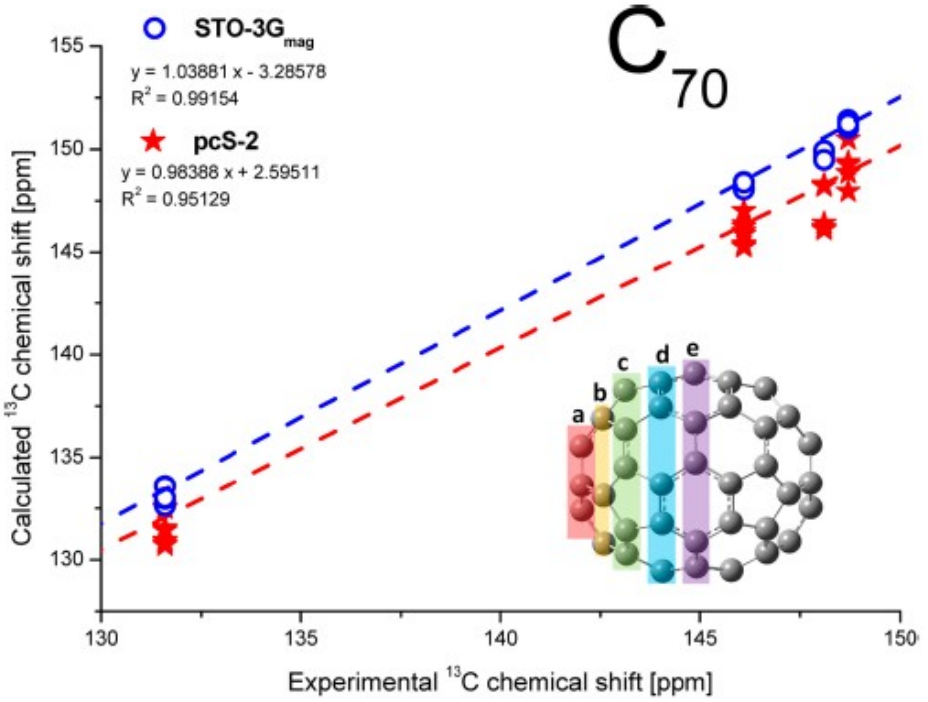


Figure 9. Performance of STO-3G$_{mag}$ and pcS-2 basis sets in predicting $C_{70}$ (top) and $C_{76}$ (bottom) $^{13}$C NMR chemical shifts (in ppm) using VSXC density functional (B3LYP/6-31G* geometry).

*Molecular Physics*, 2013
http://dx.doi.org/10.1080/00268976.2013.848301

Taylor & Francis
Taylor & Francis Group

## RESEARCH ARTICLE

# From small to medium and beyond: a pragmatic approach in predicting properties of Ne containing structures

Teobald Kupka[a,*], Michał Stachów[a], Marzena Nieradka[a], Klaudia Radula-Janik[a], Leszek Stobiński[b] and Jakub Kaminský[c]

[a]*Faculty of Chemistry, University of Opole, Opole, Poland;* [b]*Institute of Physical Chemistry, Polish Academy of Sciences, Warsaw, Poland;* [c]*Institute of Organic Chemistry and Biochemistry, Czech Academy of Sciences, Prague, Czech Republic*

(*Received 22 August 2013; accepted 19 September 2013*)

In this study, we outlined a pragmatic approach for structural studies leading to better understanding of polycarbon structures using $^{21}$Ne as a nuclear magnetic resonance (NMR) probe. $^{21}$Ne NMR parameters of a single neon atom and its dimer were predicted at the CCSD(T) level in combination with large basis sets. At a lower level of theory, an interaction of neon atom with 1,3-cyclopentadiene ring and with five- and six-membered rings in carbazole was studied using the restricted Hartree–Fock (RHF) and density functional theory (DFT) combined with smaller basis sets. The RHF and DFT modelling of neon interaction with nanosized objects were performed on cyclacenes and selected fullerenes.

**Keywords:** DFT; $^{21}$Ne NMR; dispersion interactions; carbazole; cyclacenes; fullerenes

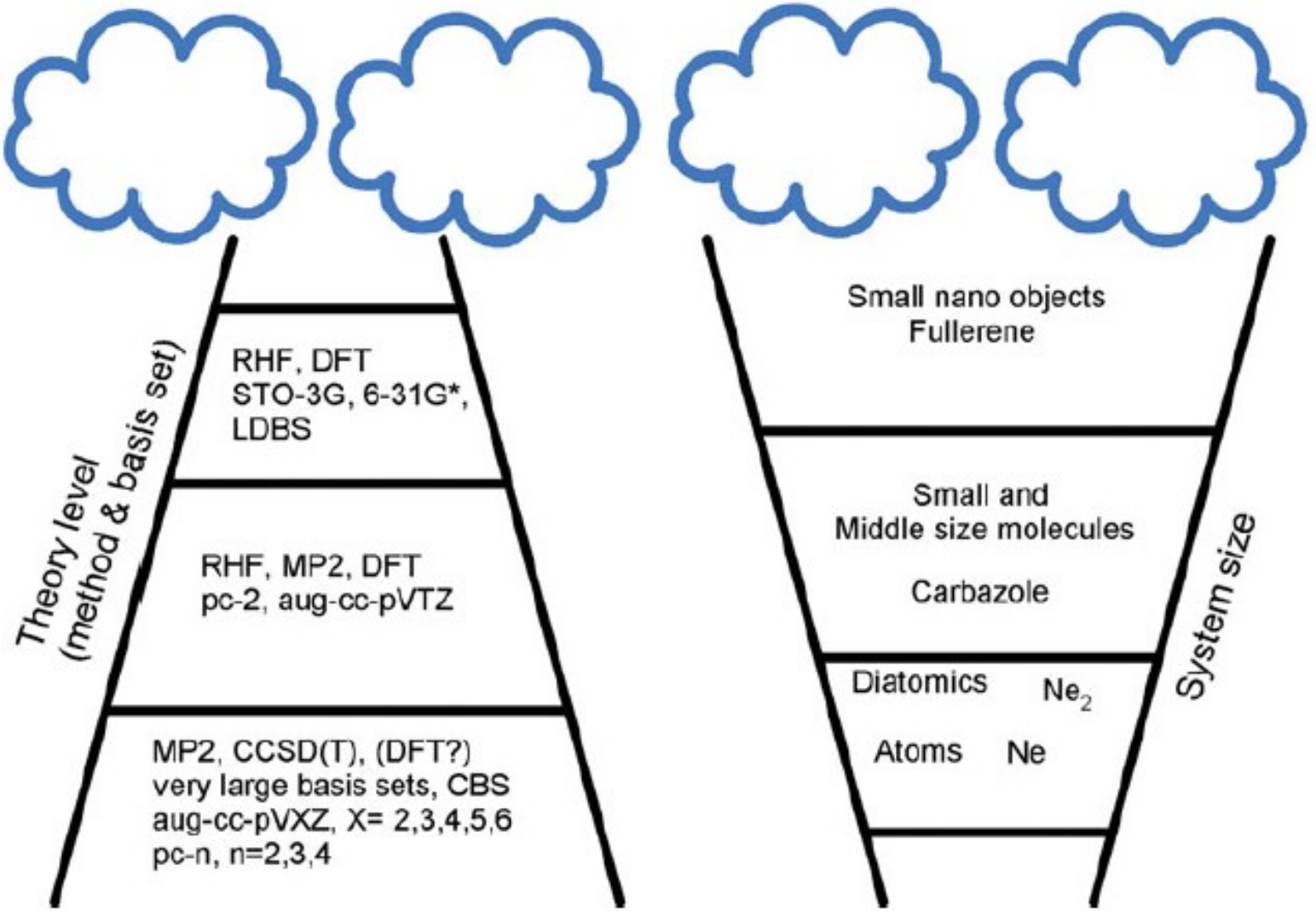


Scheme 1. 'Jacob's Ladder' explaining a compromise between system size and theory level.

Table 1. Calculated $^{21}$Ne isotropic shielding constant (ppm) for single Ne atom and $Ne_2$ dimer using several methods and basis sets.

| | Basis set | | |
|---|---|---|---|
| | Ne | | |
| Method | pcS-2 | aug-pcS-2 | aug-pcS-4 |
| RHF[a] | 554.454 | 554.421 | 552.275 |
| MP2[a] | 553.797 | 553.730 | 552.090 |
| VSXC[a] | 569.080 | 569.408 | 566.495 |
| BHandH | 554.105 | 554.052 | 551.200 |
| wB97XD | 554.597 | 554.554 | 552.332 |
| CCSD(T)[a] | 553.828 | 553.753 | 552.121 |
| | | $Ne_2$ | |
| RHF[a] | 554.027 | 554.139 | 551.904 |
| MP2[a] | 553.316 | 553.322 | 551.631 |
| VSXC[a] | 569.168 | 569.275 | 566.318 |
| BHandH | 553.522 | 553.455 | 550.579 |
| wB97XD | 554.056 | 554.065 | 551.765 |
| CCSD(T)[a] | 553.352 | 553.352 | 551.655 |

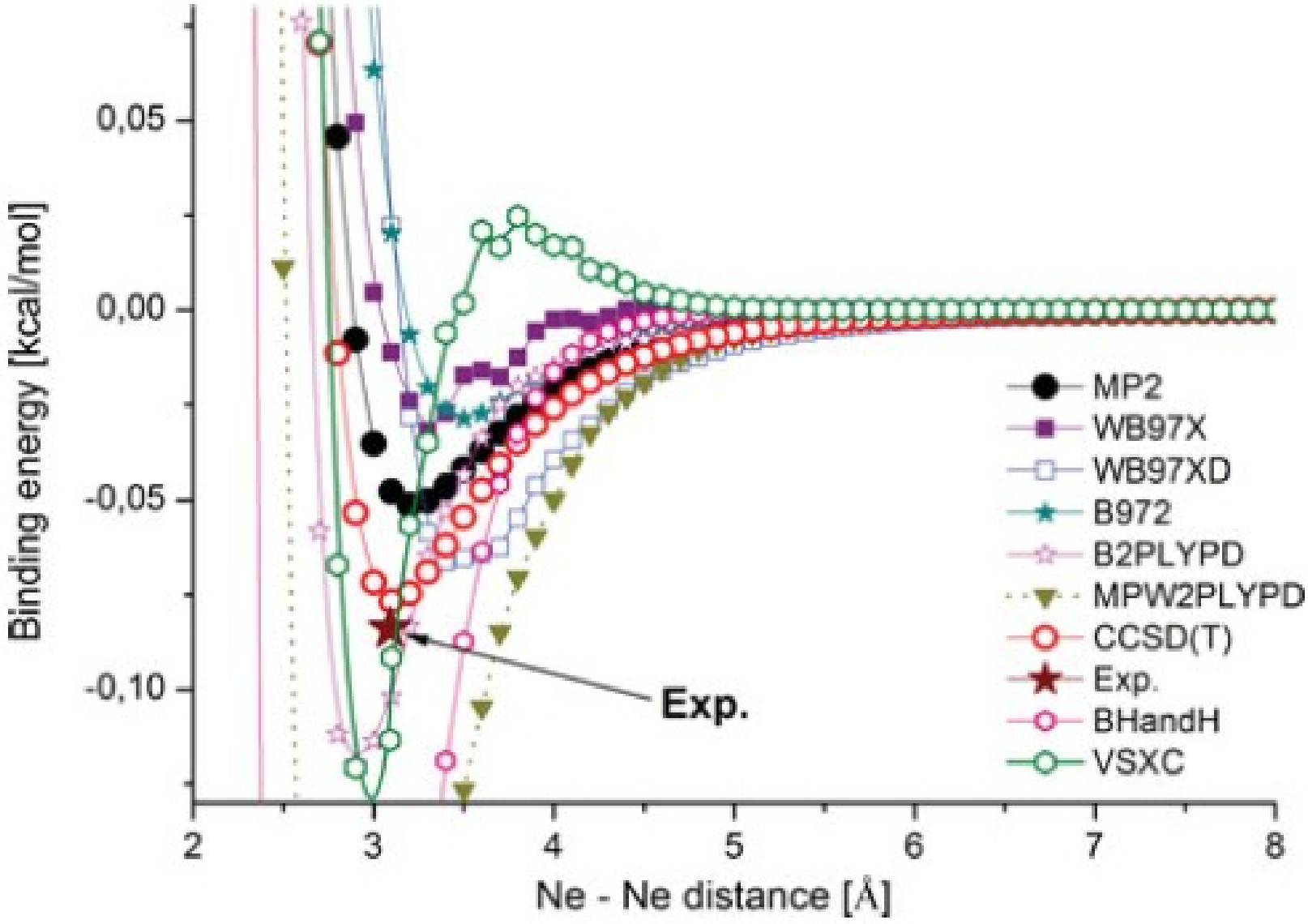


Figure 1. Dimerisation energy curve of $Ne_2$ calculated with various methods using counterpoise correction and aug-cc-pV6Z basis set.

Table 2. X–Ne separation, binding energy ($E_b$) and $^{21}$Ne chemical shift ($\delta$) of Ne atom above the centre of benzene ring at selected distances from ring plane. The aug-pcS-2 basis set was used in all calculations.

| | $E_b$ (kcal/mol) | | | | $^{21}$Ne $\delta$ (ppm) | | | | |
|---|---|---|---|---|---|---|---|---|---|
| X–Ne (Å) | MP2 | BHandH | wB97XD | VSXC | RHF | MP2 | BHandH | wB97XD | VSXC |
| 2.71[a] | −1.117 | −1.809 | 0.944 | −5.777 | −1.733 | −0.317 | 0.878 | 1.121 | 7.871 |
| 2.81[b] | −1.439 | −1.879 | 0.347 | −5.213 | −2.131 | −0.994 | −0.255 | 0.840 | 2.413 |
| 3.29[c] | −1.614 | −1.291 | −0.648 | −3.027 | −1.333 | −1.157 | −0.953 | 0.074 | 7.153 |
| 3.31[d] | −1.595 | −1.257 | −0.652 | −2.937 | −1.298 | −1.141 | −0.951 | −0.226 | 5.567 |
| 3.35[e] | −1.555 | −1.191 | −0.655 | −2.842 | −1.239 | −1.115 | −0.965 | −0.170 | 0.262 |

[a]VSXC/aug−pcS-2.
[b]BHandH/aug-pcS-2.
[c]wB97XD/aug-pcS-2.
[d]Experimental value from [15].
[e]CCSD(T)/aug-cc-pVTZ and $E_b$ is −0.45 kcal/mol, see [14].

Table 3. Predicted equilibrium distance $R_e$ (from full optimisation) between Ne and the 1,3-cyclopentadiene ring plane, binding energy ($E_b$) and $^{21}$Ne chemical shift ($\delta$) calculated with selected methods and the aug-pcS-2 basis set.

| | | | $^{21}$Ne $\delta$ (ppm) | | | | |
|---|---|---|---|---|---|---|---|
| Geometry | $R_e$ (Å) | $E_b$ (kcal/mol) | RHF | MP2 | BHandH | wB97XD | VSXC |
| VSXC | 2.74 | −5.98 | 1.058 | 1.605 | 2.042 | 2.262 | 9.812 |
| BHandH | 2.82 | −2.19 | −1.141 | −0.627 | −0.648 | −0.160 | 6.615 |
| MP2 | 3.16 | −2.06 | −1.841 | −1.687 | −2.342 | −1.926 | 1.730 |
| wB97XD | 3.46 | −0.71 | −1.603 | −1.578 | −2.383 | −2.288 | −0.710 |

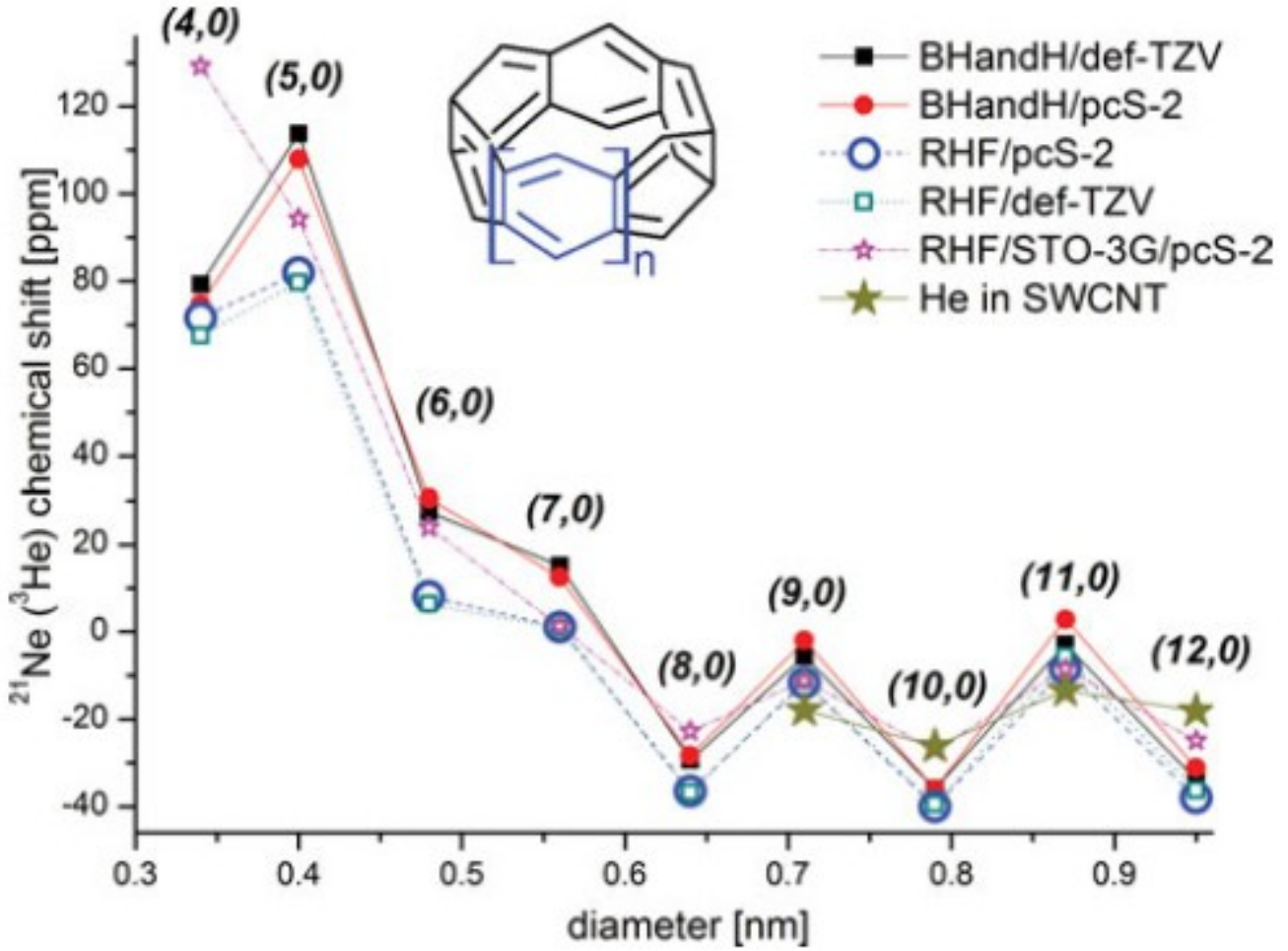


Figure 3. The RHF and BHandH calculated $^{21}$Ne chemical shift of Ne probe placed inside a cyclacenes' belt ($n = 4$–12). The pcS-2, def-TZVP and the locally dense STO-3G/pcS-2 basis sets were used and for the reader's convenience individual points are connected. For comparison, calculated $^{3}$He chemical shift of helium atom confined within *zigzag* ($n$, 0) SWCNT [19] is plotted.

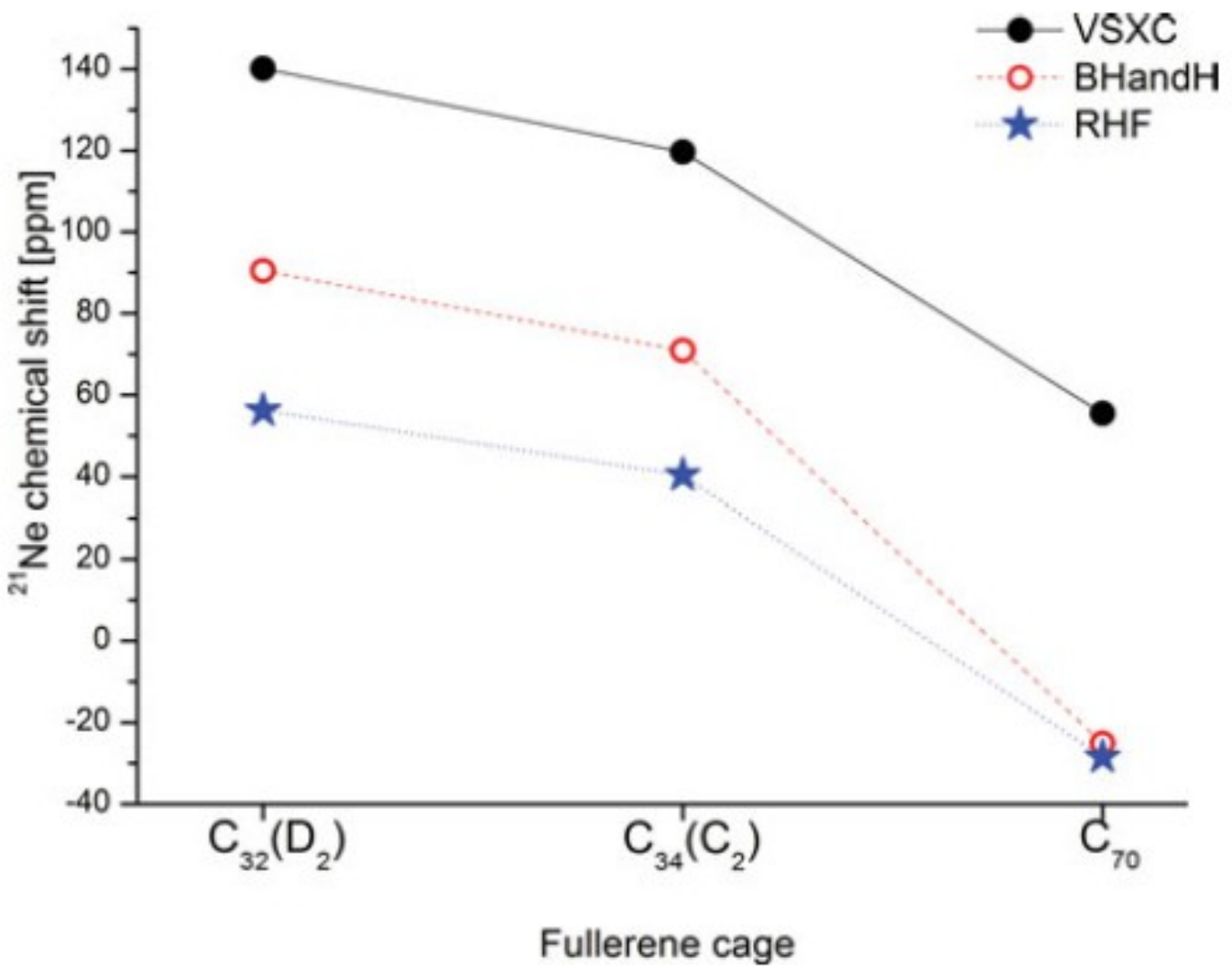


Figure 4. Calculated $^{21}$Ne chemical shift of a probe inside the fullerene using the RHF, BHandH and VSXC methods combined with the pcS-2 basis set. For the reader's convenience individual points are connected.

Received: 27 April 2013 Revised: 18 June 2013 Accepted: 18 July 2013 Published online in Wiley Online Library: 23 August 2013

(wileyonlinelibrary.com) DOI 10.1002/mrc.3999

# Modeling $^{21}$Ne NMR parameters for carbon nanosystems

**Teobald Kupka,[a]* Marzena Nieradka,[a] Jakub Kaminský[b] and Leszek Stobiński[c]**

**The potential of nuclear magnetic resonance (NMR) technique in probing the structure of porous systems including carbon nanostructures filled with inert gases is analysed theoretically using accurate calculations of neon ($^{21}$Ne) nuclear magnetic shieldings. The CBS estimates of $^{21}$Ne NMR parameters were performed for single atom, its dimer and neon interacting with acetylene, ethylene and 1,3-cyclopentadiene. Several levels of theory including restricted Hartree-Fock (RHF), Møller-Plesset perturbation theory to the second order (MP2), density functional theory (DFT) with van Voorhis and Scuseria's t-dependent gradient-corrected correlation functional (VSXC), coupled cluster with single and doubles excitations (CCSD), with single, doubles and triples included in a perturbative way (CCSD(T)) and single, doubles and tripes excitations (CCSDT) combined with polarization-consistent aug-pcS-n series of basis sets were employed. The impact of neon confinement inside selected fullerene cages used as an NMR probe was studied at the RHF/pcS-2 level of theory. A sensitivity of neon probe to the proximity of multiple CC bonds in $C_2H_2$, $C_2H_4$, $C_5H_6$ and inside $C_{28}$, $C_{30}$, $C_{32}$, $C_{34}$ and $C_{60}$ fullerenes was predicted from $^{21}$Ne NMR parameters' changes.** 

*Supporting information may be found in the online version of this article.*

**Keywords:** $^{21}$Ne NMR; GIAO NMR; molecular modeling; ordered carbon structures

**Table 1.** Calculated $^{21}$Ne isotropic shielding constant (ppm) for single Ne atom and $Ne_2$ dimer using several methods and aug-pcS-n basis sets

| Method | Basis set | | | | | | | |
|---|---|---|---|---|---|---|---|---|
| | **Ne** | | | | | | | |
| | pcS-2 | pcS-3 | pcS-4 | CBS | aug-pcS-2 | aug-pcS-3 | aug-pcS-4 | CBS |
| HF | 554.454 | 552.269 | 552.275 | 552.277 | 554.421 | 552.270 | 552.275 | 552.277 |
| MP2 | 553.797 | 552.021 | 552.093 | 552.123 | 553.730 | 552.015 | 552.090 | 552.122 |
| VSXC | 569.080 | 566.554 | 566.481 | 566.451 | 569.408 | 566.537 | 566.495 | 566.477 |
| CCSD | 553.869 | 552.097 | 552.177 | 552.211 | 553.806 | 552.092 | 552.176 | 552.211 |
| CCSD(T) | 553.828 | 552.044 | 552.123 | 552.156 | 553.752 | 552.038 | 552.121 | 552.156 |
| CCSDT | 553.829 | 552.045 | 552.124 | 552.157 | 553.753 | 552.039 | 552.122 | 552.157 |
| | **$Ne_2$** | | | | | | | |
| HF | 554.027 | 551.890 | 551.905 | 551.907 | 554.139 | 551.295 | 551.904 | 552.160 |
| MP2 | 553.316 | 551.561 | 551.626 | 551.768 | 553.322 | 551.584 | 551.631 | 551.650 |
| VSXC | 569.168 | 566.581 | 566.510 | 566.480 | 569.275 | 566.458 | 566.318 | 566.260 |
| CCSD | 553.394 | 551.655 | 551.732 | 551.764 | 553.421 | 551.666 | 551.727 | 551.753 |
| CCSD(T) | 553.352 | 551.590 | 551.662 | 551.692 | 553.352 | 551.598 | 551.655 | 551.679 |
| CCSDT | 553.352 | 551.590 | [b] | | 553.351 | [b] | [b] | |

[a] Experimental Ne-Ne distance of 3.091 Å from Ref. [35].

[b] Convergence problems.

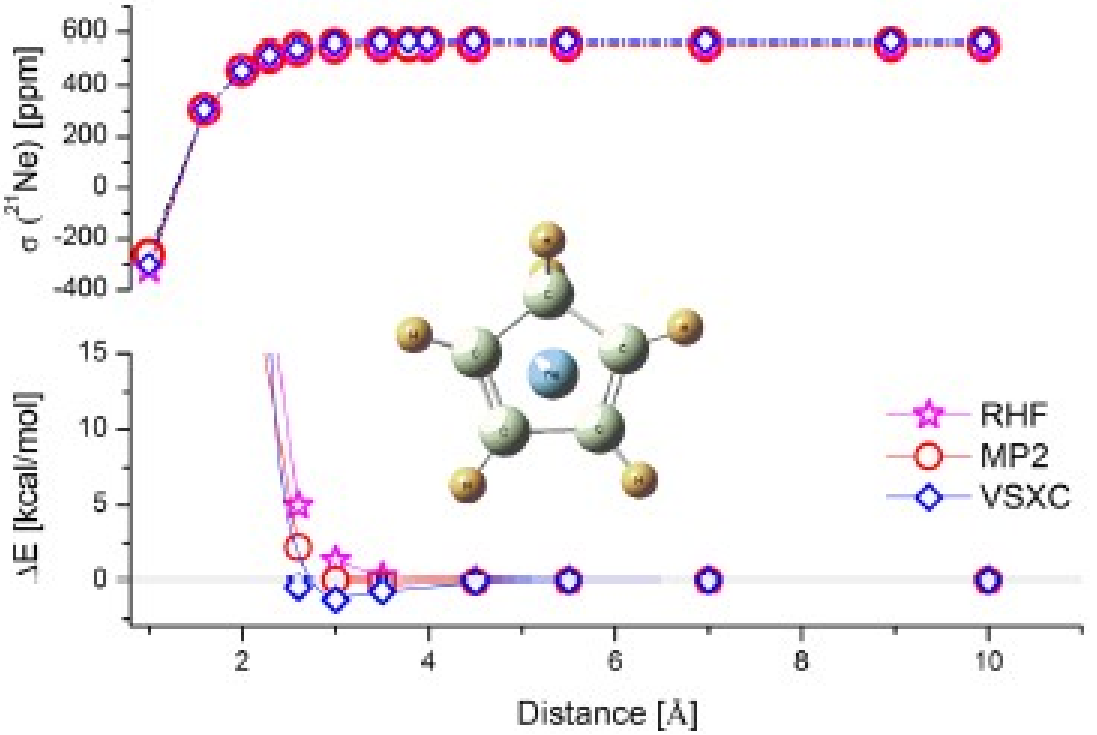

**Table 2.** The RHF/pcS-2 $^{21}$Ne NMR parameters (in ppm, relative to gas value[a]) of a single Ne atom encapsulated in a fullerene cage

| Molecule | Shift tensor components | | | Isotropic shielding | Shielding anisotropy | Chemical shift [ppm] |
|---|---|---|---|---|---|---|
| | $\sigma_{xx}$ | $\sigma_{yy}$ | $\sigma_{zz}$ | $\sigma_{iso}$ | $\Delta\sigma$ | $\delta$ |
| Ne gas | 554.454 | 554.454 | 554.454 | 554.454 | 0.000 | 0.000 |
| $Ne_2$ | 552.137 | 552.137 | 552.546 | 552.273 | 0.409 | 2.181 |
| Ne@$C_{28}(T_d)$ | 318.120 | 397.375 | 615.509 | 443.668 | 257.762 | 110.786 |
| Ne@$C_{30}(C_2)$ | 483.793 | 515.756 | 538.126 | 512.558 | 38.351 | 41.896 |
| Ne@$C_{30}(D_2)$ | 486.960 | 534.520 | 598.889 | 540.123 | 88.173 | 14.331 |
| Ne@$C_{32}(C_2)$ | 515.436 | 546.196 | 556.229 | 539.287 | 31.672 | 15.167 |
| Ne@$C_{32}(D_2)$ | 456.879 | 489.370 | 548.466 | 498.238 | 93.416 | 56.216 |
| Ne@$C_{34}(C_2)$ | 485.840 | 518.704 | 537.635 | 514.060 | 86.386 | 40.394 |
| Ne@$C_{60}(I_h)$ | 567.599 | 567.603 | 567.603 | 567.602 | 0.003 | −13.148 |

[a]Results for single atom representing low pressure gas and neon dimer are given for comparison (for some systems $T_d$, $C_2$, $D_2$ and $I_h$ symmetry is indicated)

Received: 12 May 2013 Revised: 10 July 2013 Accepted: 10 July 2013 Published online in Wiley Online Library: 6 August 2013

(wileyonlinelibrary.com) DOI 10.1002/mrc.3992

# Halogen effect on structure and $^{13}C$ NMR chemical shift of 3,6-disubstituted-*N*-alkyl carbazoles

**Klaudia Radula-Janik,[a] Teobald Kupka,[a]* Krzysztof Ejsmont,[a] Zdzislaw Daszkiewicz[a] and Stephan P. A. Sauer[b]***

**Structures of selected 3,6-dihalogeno-*N*-alkyl carbazole derivatives were calculated at the B3LYP/6-311++G(3df,2pd) level of theory, and their $^{13}C$ nuclear magnetic resonance (NMR) isotropic shieldings were predicted using density functional theory (DFT). The model compounds contained 9H, *N*-methyl and *N*-ethyl derivatives. The relativistic effect of Br and I atoms on nuclear shieldings was modeled using the spin–orbit zeroth-order regular approximation (ZORA) method. Significant heavy atom shielding effects for the carbon atom directly bonded with Br and I were observed (~−10 and ~−30 ppm while the other carbon shifts were practically unaffected). The decreasing electronegativity of the halogen substituent (F, Cl, Br, and I) was reflected in both nonrelativistic and relativistic NMR results as decreased values of chemical shifts of carbon atoms attached to halogen (C3 and C6) leading to a strong sensitivity to halogen atom type at 3 and 6 positions of the carbazole ring. The predicted NMR data correctly reproduce the available experimental data for unsubstituted *N*-alkylcarbazoles.** 

*Supporting information may be found in the online version of this article.*

**Keywords:** carbazole; $^{13}C$ NMR; GIAO NMR; halogen substituent; relativistic effect; HALA

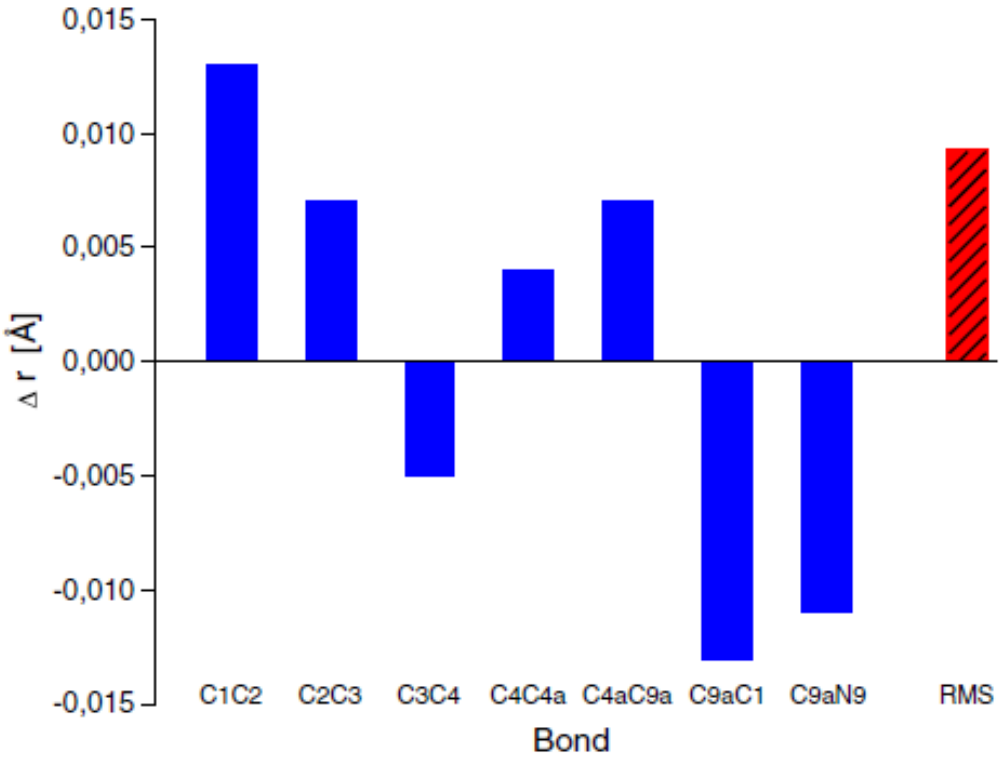


**Figure 2.** Deviation of bond lengths (Δr) from experimental data[74] for 9H-carbazole (B3LYP/6-311++G(3df,2pd) results).

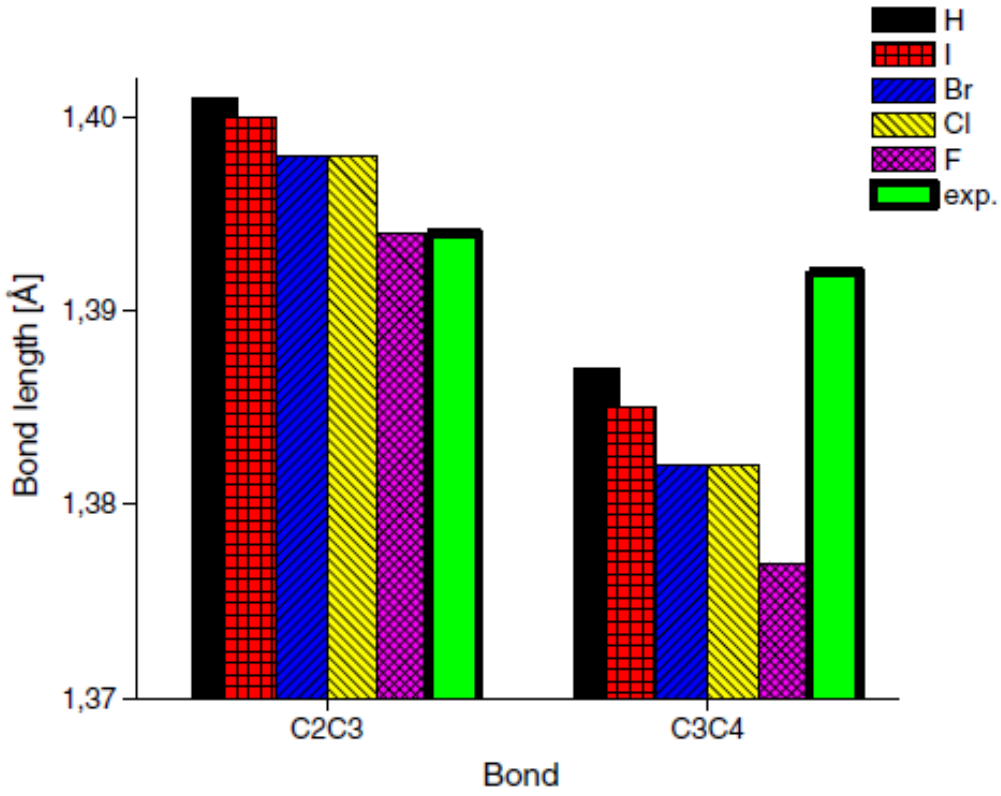


**Figure 3.** Selected bond lengths variations upon changing substituent X (halogen) for 9H-carbazole predicted at B3LYP/6-311++G(3df,2pd) level of theory.

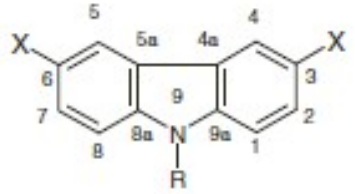


R= H, C(10)$H_3$, C(10)$H_2$C(11)$H_3$

X= H, F, Cl, Br, I

**Figure 1.** Atom numbering of carbazole and its selected 3,6-disubstituted derivatives.

**Table 1.** Comparison of nonrelativistic[a] VSXC/STO-3$G_{mag}$, KT2/DZP, and relativistic spin–orbit ZORA (KT2/DZP) calculated chemical shifts (in ppm) for 9H, *N*-methylcarbazole and *N*-ethylcarbazole

| X=H | Chemical shift [ppm] | | | | | | | | |
|---|---|---|---|---|---|---|---|---|---|
| | 9H | | | N—Me | | | N—Et | | |
| Carbon | NR1 | NR2 | ZORA | NR1 | NR2 | ZORA | NR1 | NR2 | ZORA |
| C1 | 110.4 | 110.6 | 110.6 | 108.0 | 110.1 | 110.1 | 107.3 | 110.3 | 110.3 |
| C2 | 126.0 | 126.5 | 126.5 | 125.9 | 126.4 | 126.4 | 126.0 | 126.5 | 126.5 |
| C3 | 119.9 | 121.0 | 121.0 | 119.7 | 120.6 | 120.6 | 119.8 | 120.6 | 120.6 |
| C4 | 120.7 | 121.3 | 121.3 | 120.8 | 121.1 | 121.1 | 121.2 | 121.3 | 121.3 |
| C4a | 127.2 | 126.2 | 126.2 | 127.2 | 126.5 | 126.5 | 127.3 | 126.7 | 126.8 |
| C9a | 141.4 | 140.4 | 140.4 | 143.4 | 142.9 | 142.8 | 142.1 | 142.1 | 142.0 |

[a]Abbreviated as NR1 and NR2, respectively.

**Table 2.** Comparison of nonrelativistic VSXC/STO-3G$_{mag}$ and KT2/DZP and relativistic spin–orbit ZORA (KT2/DZP) calculated chemical shifts (in ppm) for 3,6-dihalogeno-9H, *N*-methylcarbazoles and *N*-ethylcarbazoles

| X=F | Chemical shift [ppm] | | | | | | | | |
|---|---|---|---|---|---|---|---|---|---|
| | 9H | | | N—Me | | | N—Et | | |
| Carbon | NR1 | NR2 | ZORA | NR1 | NR2 | ZORA | NR1 | NR2 | ZORA |
| C1 | 111.0 | 111.0 | 111.1 | 108.6 | 110.6 | 110.6 | 107.9 | 110.8 | 110.8 |
| C2 | 114.6 | 115.8 | 115.8 | 114.4 | 115.6 | 115.6 | 114.4 | 115.6 | 115.6 |
| C3 | 163.9 | 168.8 | 168.4 | 164.0 | 168.8 | 168.4 | 163.9 | 168.7 | 168.3 |
| C4 | 106.9 | 108.1 | 108.1 | 107.1 | 108.0 | 108.0 | 107.5 | 108.1 | 108.2 |
| C4a | 127.3 | 126.7 | 126.8 | 126.9 | 126.7 | 126.7 | 127.0 | 126.9 | 127.0 |
| C9a | 138.1 | 137.9 | 137.9 | 140.1 | 140.3 | 140.2 | 138.8 | 139.4 | 139.4 |
| X = Cl | | | | | | | | | |
| C1 | 111.1 | 111.4 | 111.4 | 108.8 | 110.9 | 111.0 | 108.1 | 111.1 | 111.2 |
| C2 | 126.6 | 128.1 | 128.1 | 126.4 | 127.8 | 127.8 | 126.5 | 127.9 | 127.9 |
| C3 | 139.7 | 142.4 | 140.2 | 139.6 | 142.1 | 139.9 | 139.4 | 142.0 | 139.8 |
| C4 | 120.3 | 121.7 | 121.7 | 120.5 | 121.5 | 121.6 | 120.8 | 121.7 | 121.8 |
| C4a | 127.1 | 126.8 | 126.9 | 126.8 | 126.9 | 127.0 | 127.0 | 127.1 | 127.2 |
| C9a | 139.4 | 138.9 | 138.9 | 141.4 | 141.4 | 141.3 | 140.2 | 140.6 | 140.5 |
| X = Br | | | | | | | | | |
| C1 | 111.4 | 111.8 | 111.9 | 109.1 | 111.3 | 111.5 | 108.4 | 111.5 | 111.7 |
| C2 | 129.5 | 131.0 | 131.0 | 129.3 | 130.8 | 130.8 | 129.4 | 130.8 | 130.8 |
| C3 | **137.6** | **141.0** | **130.3** | **137.5** | **140.6** | **130.1** | **137.3** | **140.5** | **130.1** |
| C4 | 123.6 | 125.0 | 125.2 | 123.8 | 124.8 | 125.0 | 124.1 | 125.0 | 125.2 |
| C4a | 127.5 | 127.2 | 127.5 | 127.2 | 127.3 | 127.6 | 127.3 | 127.6 | 127.9 |
| C9a | 139.7 | 139.2 | 139.0 | 141.7 | 141.6 | 141.5 | 140.5 | 140.9 | 140.7 |
| X = I | | | | | | | | | |
| C1 | 111.8 | 111.8 | 112.1 | 109.5 | 111.4 | 111.7 | 108.9 | 111.7 | 111.9 |
| C2 | 134.0 | 135.6 | 135.7 | 133.9 | 135.4 | 135.5 | 133.9 | 135.4 | 135.6 |
| **C3** | **128.0** | **126.8** | **99.0** | **127.7** | **126.4** | **98.9** | **127.5** | **126.3** | **98.8** |
| C4 | 128.7 | 130.1 | 131.0 | 128.8 | 129.9 | 130.7 | 129.2 | 130.1 | 130.9 |
| C4a | 127.8 | 127.2 | 127.5 | 127.6 | 127.4 | 127.7 | 127.7 | 127.6 | 128.0 |
| C9a | 140.1 | 139.2 | 138.7 | 142.1 | 141.6 | 141.2 | 140.9 | 140.9 | 140.4 |

In bold are shown data affected by heavy atom on light atom effect.

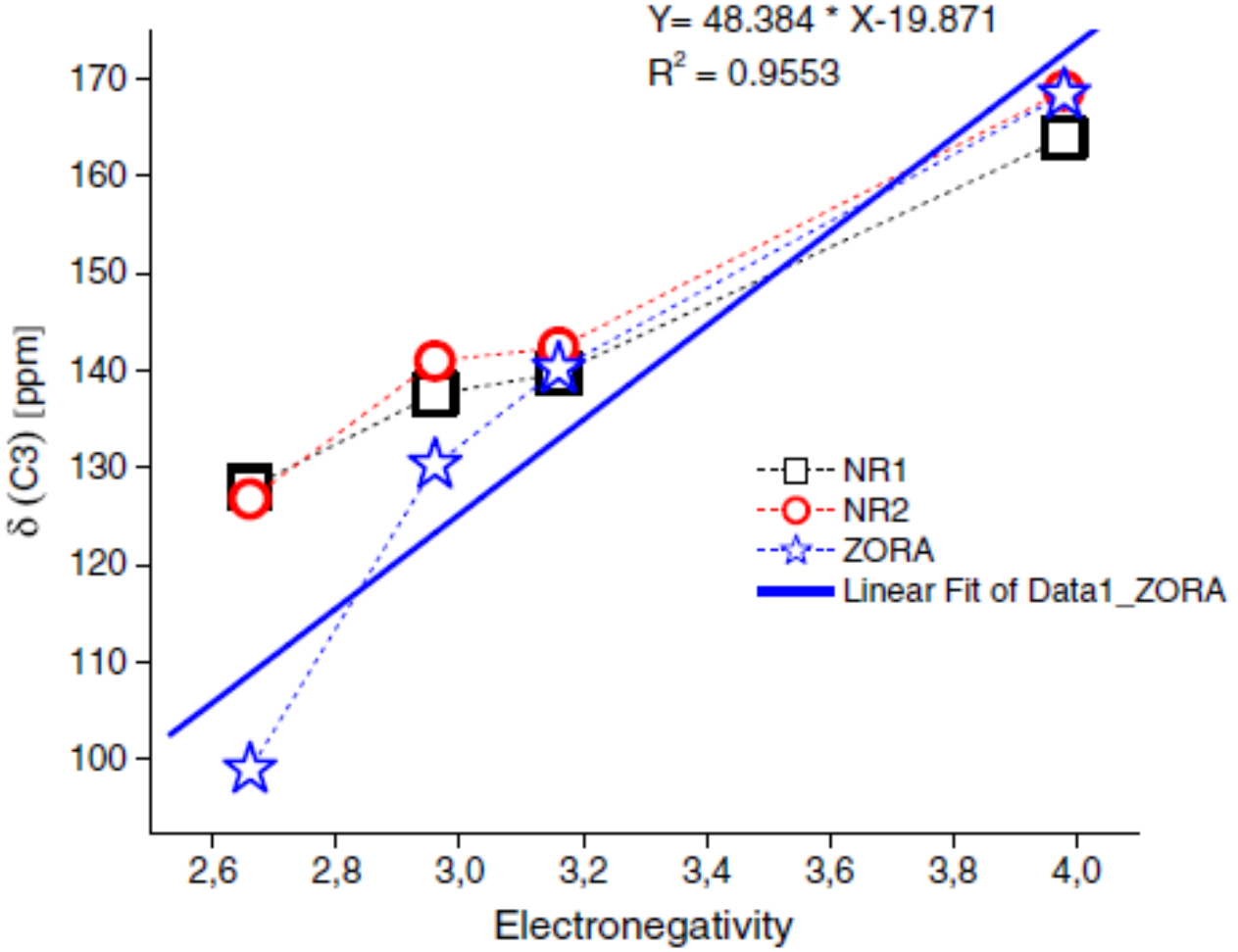


**Figure 5.** Effect of electronegativity on the C3 chemical shifts calculated at nonrelativistic VSXC/STO-3G$_{mag}$ and KT2/DZP and relativistic spin–orbit ZORA (KT2/DZP) calculated chemical shifts (in ppm) for 3,6-dihalogeno-9H-carbazole.

**Badania koncentrowały się na przewidywaniu struktury geometrycznej oraz wybranych parametrów spektroskopowych (NMR, IR, Raman) małych molekul modelowych, jednościennych nanorurek węglowych (SWCNT) przed i po funkcjonalizowaniu oraz fulerenów.**

**Ponadto przeprowadzono szczegółową analizę konformacyjną (teoretyczną i eksperymentalną) wybranych dehydropeptydów i ich oddziaływań z lecytyną.**

**SWCNT i fullereny: podstawienie końca grupami -OH i –COOH, $^{3}$He i $^{21}$Ne**

**Karbazole (obliczenia relatywistyczne do NMR (ZORA)**

**NMR: nowe bazy, CBS, gazy szlachetne jako sondy NMR**

**Dehydropeptydy (peptydomimetyki)**

**Obliczenia - Gausian 09; metody - DFT, HF; MP2, CC**
**CFOUR (CCSD(T))**

# Wnioski:

1. Owocna kontynuacja testowania metody CBS NMR (stałe ekranowania i stałe sprzężeń spinowo-spinowych).

2. Zastosowanie CBS do wyznaczania innych parametrów molekularnych i spektroskopowych (struktura geometryczna, częstości drgań harmonicznych i anharmonicznych

3. Obliczenia DFT dla SWCNTs i fulerenów. Gazy szlachetne jako sondy NMR

4. Skuteczna modyfikacja struktury dehydropeptydów (eksperyment i teoria)

# Podziękowania:

1. **WCSS Wrocław** (oprogramowanie,sprzęt komputerowy i pomoc techniczna).

2. Uniwersytet Opolski, Wydział Chemii

# Z Kraju Ryżu, Herbaty i Tajfunów do ... Wrocławia’2014

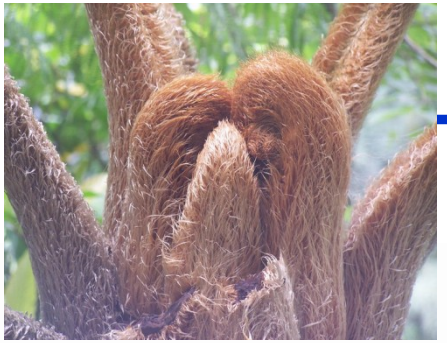


# Dziękuję za uwagę